Peer-reviewed version available at Water 2016, 8, 389; doi:10.3390/w8090389

Article

The Impact of Climate Change on Reservoir Inflows Using Multi Climate-Model under RCPs' Including Extreme Events—A Case of Mangla Dam, Pakistan

Muhammad Babur [1,*], Mukand Singh Babel [1], Sangam Shrestha [1], Akiyuki Kawasaki [1] and Nitin K. Tripathi [2]

[1] Water Engineering and Management Program, School of Engineering and Technology, Asian Institute of Technology, P.O. Box 4, Klong Luang, Pathumthani 12120, Thailand; msbabel@ait.asia (M.S.B.); sangam@ait.asia (S.S.); kawasaki@ait.asia (A.K.)

[2] Remote Sensing and GIS, School of Engineering and Technology, Asian Institute of Technology, P.O. Box 4, Klong Luang, Pathumthani 12120, Thailand; nitinkt@ait.ac.th

* Correspondence: st114348@ait.ac.th; Tel.: +66-863-002-849; Fax: +66-992-098-117

Abstract: Assessment of extreme events and climate change on reservoir inflow is important for water and power stressed countries. Projected climate is subject to uncertainties related to climate change scenarios and Global Circulation Models (GCMs'). Extreme climatic events will increase with the rise in temperature as mentioned in the AR5 of the IPCC. This paper discusses the consequences of climate change that include extreme events on discharge. Historical climatic and gauging data were collected from different stations within a watershed. The observed flow data was used for calibration and validation of SWAT model. Downscaling was performed on future GCMs' temperature and precipitation data, and plausible extreme events were generated. Corrected climatic data was applied to project the influence of climate change. Results showed a large uncertainty in discharge using different GCMs' and different emissions scenarios. The annual tendency of the GCMs' is bi-vocal: six GCMs' projected a rise in annual flow, while one GCM projected a decrease in flow. The change in average seasonal flow is more as compared to annual variations. Changes in winter and spring discharge are mostly positive, even with the decrease in precipitation. The changes in flows are generally negative for summer and autumn due to early snowmelt from an increase in temperature. The change in average seasonal flows under RCPs' 4.5 and 8.5 are projected to vary from -29.1 to 130.7% and -49.4 to 171%, respectively. In the medium range (RCP 4.5) impact scenario, the uncertainty range of average runoff is relatively low. While in the high range (RCP 8.5) impact scenario, this range is significantly larger. RCP 8.5 covered a wide range of uncertainties, while RCP 4.5 covered a short range of possibilities. These outcomes suggest that it is important to consider the influence of climate change on water resources to frame appropriate guidelines for planning and management.

Keywords: climate change; GCMs'; RCPs'; downscaling; temperature; precipitation; extreme events; SWAT; discharge

1. Introduction

Global mean temperature is estimated to climb up by 0.6°C [1] over the course of the 20th century. Climate models estimate [2-8] that the global average temperature is likely to increase 4.0°C by the conclusion of the 21st century [9]. Reliable prediction of climate is pre-requisite to comprehend the impacts of climate change [10].

Various authors used SRES scenarios for climate change impact studies, [11-15] nowadays those scenarios have become outdated. Most of the research to date in the Jhelum and Upper Indus Basin have utilized a few GCMs' under SRES scenarios for climate change impact studies [16-22]. The SRES scenarios exaggerate resource accessibility and are unlikely on upcoming production outputs from fossil fuels [23]. RCPs' are new scenarios and these overcome the shortcoming of SRES scenarios. The

RCPs' are not linked with exclusive socioeconomic assumptions or emissions scenarios. However, these are based on the groupings of economic, technological, demographic, policy, and future institutional challenges of mitigation and adaptation. Another benefit of RCPs' is its better resolution that helps in performing regional and local comparative studies [23].

The uncertainties in future climate originate due to internal climate variability, model uncertainty, and scenario uncertainty [24]. The specific processes and feedbacks are major reasons of model uncertainty. While, incomplete knowledge of external factors affecting the climate system are the major sources of scenario uncertainty [24,25].

Majone et al. (2016) reported a rise in the average temperature of the Noce basin, which is located in Italy, from 2 to 4°C depends on the climate model. The study indicated a rise in an annual average precipitation from 2 to 6% with more changes in winter and autumn. The water yield showed an increase under SRES scenarios [26].

Akhtar et al. (2008) observed trends of rainfall in three decades (1961-1999) for Upper Indus Basin (UIB) nearby Jhelum Basin. It was stated that the values of decadal escalation in rainfall at the major station of UIB i.e. Skardu, Shahpur, and Dir climate stations as 22, 103 and 120mm, respectively [27]. Furthermore, the mean annual temperature and mean annual precipitation will rise in UIB in the 21st century from 0.3 to 4.8°C, 19 to 113%, respectively [27]. In that study, a few GCMs' were used under SRES scenarios. The gap in literature was found, and to fill that gap this study is much needed.

This study aims to answer following major questions: What will be a probable climate of Mangla watershed? How inflow into Mangla Reservoir will change because of climate change using GCMs' under RCPs' and extreme events? The selection of GCMs' intensely affects the expected changes of climatological parameters [28]. In this paper, seven GCMs': BCC-CSM 1.1-m, CCSM4, CSIRO BOM ACCESS1-0, GFDL-CM3, MIROC5, MRI-CGCM3, and UKMO-HadGEM2 under two RCPs' 4.5 and 8.5 were selected to simulate future discharge using hydrological model SWAT. Description of the study area and data are specified in sections 2 and 3 of this paper. A short description of the hydrological model and the methods employed for the analysis of climate change and streamflow is given in section 3 and 4. Results/discussion and conclusions are given in sections 5 and 6 respectively. The first novelty of this study is the use of a wide range of GCMs' to cover uncertainties of future climate. The second novelty of this research is the use of new scenarios RCPs' to cover the uncertainty regarding emission scenarios in all three future time slices. The third novelty is that; this study also quantifies the impact of extreme events on discharge. The fourth novelty is that; the impact of climatic parameters on flows is quantified. This study will be useful to planners and decision makers when planning and applying suitable water management practices for water resources and hydropower to adapt the impacts of climate change including extreme events.

2. Study Area

Mangla Basin is situated in the northeastern part of Pakistan with the total watershed area of 33,470km^2. The study area is divided into seven sub-basins (Kunhar, Neelum, Upper Jhelum, Lower Jhelum, Poonch, Kanshi, and Kahan) as presented in Figure 1. The catchment areas of the sub-basins are; 2,632km^2, 7,421km^2, 14,400km2, 2,974km^2, 4,436km^2, 1,303km^2, and 324 km^2, respectively. The slope is divided into three classes 0-3%, 8-30%, and > 30% are undulating lands, steep slopes and mountainous land [29]. Major slopes of Mangla watershed are mountainous land and steep slopes.

A principal amount of water enters in the Mangla reservoir from March to August. Generally, in May, the maximum quantity of water comes in the reservoir. During, October to February very less flow comes into the reservoir, mostly less than 400m^3/sec. Due to snowmelt, the flow of water starts increasing in March and gains absolute peak in the middle of May. More than 75% of the flow comes in the reservoir from March to August. While, in the remaining six months less than 25% flows reaches in the reservoir.

Due to hydrological (a reasonable amount of flow) and topographical (narrow garage, high head availability) characteristics, hydropower projects have been developed in this area. Mangla power station is one of the prominent HPP in this region [30], and it contributes almost 30% of the hydel energy of Pakistan. Mangla dam is the 12th largest dam in the world [31].

Preprints (www.preprints.org) | NOT PEER-REVIEWED | Posted: 24 August 2016 doi:10.20944/preprints201608.0200.v1

Peer-reviewed version available at Water 2016, 8, 389; doi:10.3390/w8090389

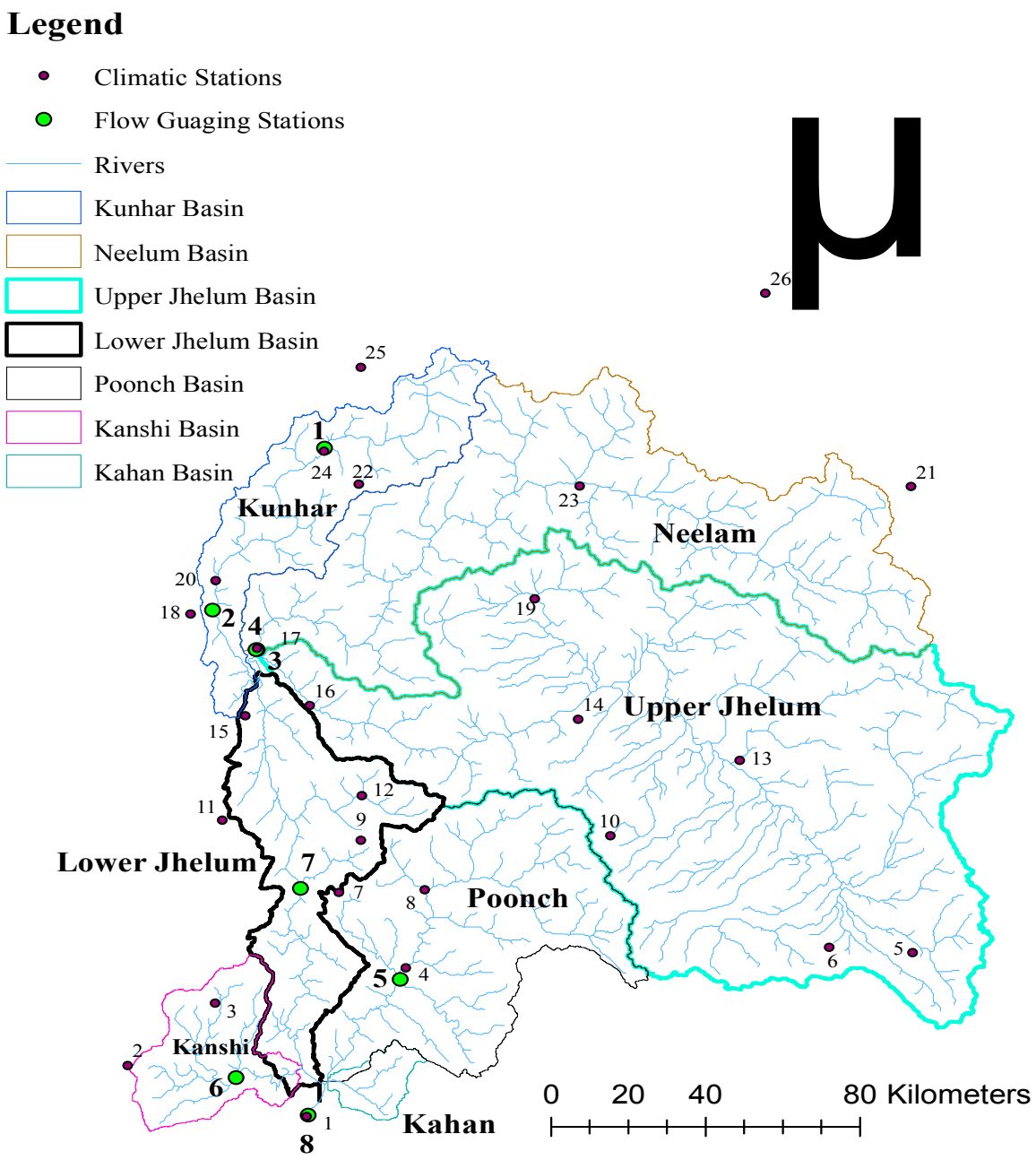

Figure 1. The Mangla River basin showing climatic stations in red dots and flow gauging stations in green dots and sub-basins.

Mean monthly temperature and precipitation in Mangla watershed and sub-basins are specified in Figure 2. In general, precipitation distribution in the watershed is bi-modular, first, larger peak comes in March in the form of snowfall and second lower peak comes in July in the form of monsoon rainfall. During observed period (1979-2010), the highest amount of precipitation happens in the northern hilly part of the Kunhar sub-basin. There is a noteworthy spatial variation in precipitation over the Mangla watershed. The average annual precipitation in the northern and the southern parts are 1893mm, and 846mm, respectively. About half of the annual precipitation for northern area occurs from December to March in the form of snow. Moreover, to the rain and snowfall, permanent glaciers are the sources of stream flow. The temperature in the watershed varies extremely. On one hand, in the northern part of the basin, the temperature regularly drops below 0°C from December to March. On the other hand, in the southern part of the basin, temperature can touch 50°C in June.

Preprints (www.preprints.org) | NOT PEER-REVIEWED | Posted: 24 August 2016 doi:10.20944/preprints201608.0200.v1

Peer-reviewed version available at Water 2016, 8, 389; doi:10.3390/w8090389

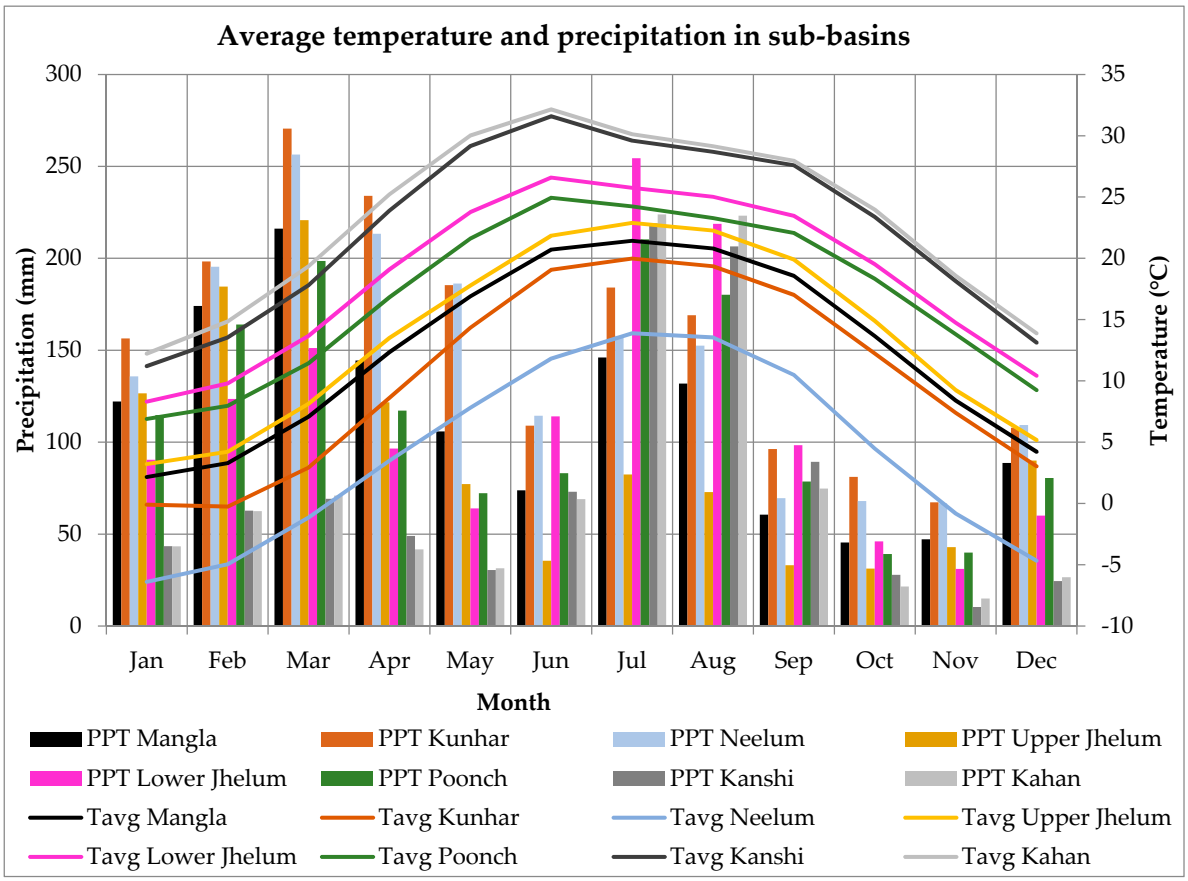

Figure 2. Mean monthly temperature and precipitation in Mangla watershed and sub-basins.

3. Data

3.1 Observed data

3.1.1. Meteorological Data

The observed daily meteorological data were collected from the Pakistan Meteorological Department (PMD), Surface Water Hydrology Project (SWHP) of Water and Power Development Authority (WAPDA) Pakistan, Indian Meteorological Department (IMD), and National Centers for Environmental Prediction's Climate Forecast System Reanalysis (CFSR). The SWHP is mainly for measurement of discharge, but also observes certain climatic variables namely precipitation and temperature. The data collected includes daily, Tmax and Tmin, precipitation, solar radiation, wind speed and relative humidity. An inventory of meteorological stations is presented in Table 1. The location of the climatological stations is displayed in Figure 1. If only observed weather station data are utilized, then amount precipitation in three sub-basins is less than total flows. Practically, it is impossible. This means that installed weather stations are not sufficient to represent the climate of mountainous watershed.

CFSR data can be used in the data-scarce region [32,33]. The observed climatic data were missing in some stations and does not cover the entire basin, that is why CFSR data were used in the Mangla Basin to overcome this limitation. Data of six out of 26 stations used in this study is taken from CFSR database and other five stations missing data for the significant period were filled with CFSR data. Daily precipitation, Tmax, Tmin, solar radiation, wind speed and relative humidity, having a resolution of 0.50° x 0.50° is available from 1979 to 2011on website (http://globalweather.tamu.edu).

Table 1. Inventory of climate stations.

Sr. No.	Name	Latitude N	Longitude E	Elevation m, MSL	Data Source	observation period
1	Mangla	33.12	73.63	282	PMD	1960-2010
2	Gujjar Khan	33.25	73.13	547	PMD	1960-2010
3	Kallar	33.42	73.37	518	PMD	1960-2010
4	Rehman Br.(Kotli)	33.52	73.9	614	PMD	1960-2010
5		33.565	75.313	2317	CFSR data	1979-2010
6		33.58	75.08	1690	CFSR data	1979-2010
7	Palandri	33.72	73.71	1402	SWHP	1962-2010
8	Sehr kakota	33.73	73.95	915	PMD	1961-2010
9	Rawalakot	33.86	73.77	1676	SWHP	1960-2010
10		33.877	74.468	2154	CFSR data	1979-2010
11	Murree	33.91	73.38	2213	SWHP	1960-2010
12	Bagh	33.98	73.77	1067	SWHP	1961-2010
13	Srinagar	34.08	74.83	1587	IMD	1892-2010
14		34.189	74.375	1821	CFSR data	1979-2010
15	Domel	34.19	73.44	702	SWHP	1961-2010
16	Gharidopatta	34.22	73.62	814	PMD	1954-2010
17	Muzaffarabad	34.37	73.47	686	SWHP	1962-2010
18	Shinkiari	34.46	73.28	1050	PMD	1961-2010
19	Kupwara	34.51	74.25	1609	IMD	1960-2010
20	Balakot	34.55	73.35	995.4	PMD	1961-2010
21		34.813	75.313	4360	CFSR data	1979-2010
22		34.813	73.75	3720	CFSR data	1979-2010
23		34.813	74.375	2612	CFSR data	1979-2010
24	Naran	34.9	73.65	2362	PMD	1961-2010
25		35.126	73.75	3284	CFSR data	1979-2010
26	Astore	35.33	74.9	2168	PMD	1954-2010

Preprints (www.preprints.org) | NOT PEER-REVIEWED | Posted: 24 August 2016 doi:10.20944/preprints201608.0200.v1

Peer-reviewed version available at Water 2016, 8, 389; doi:10.3390/w8090389

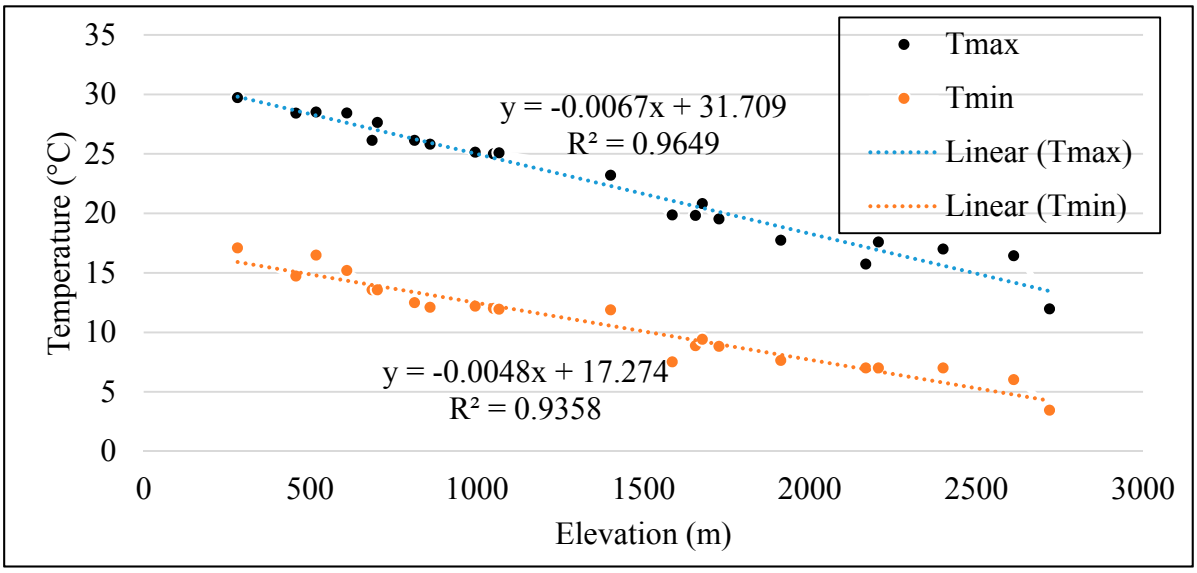

Figure 3. Relationship between temperature and elevations of the Jhelum Basin.

The temperature data from observed climatological gauges were used to estimate the lapse rate for the Jhelum River Basin. With the increase in elevation, temperature follows a negative trend. The Lapse rate for the basin was calculated based on the relationship between the average daily temperature and the altitude of the climate stations. Figure 4 displays a very good correlation between temperature and elevation. The Lapse rate for the study area is -6.7°C/km increase in elevation.

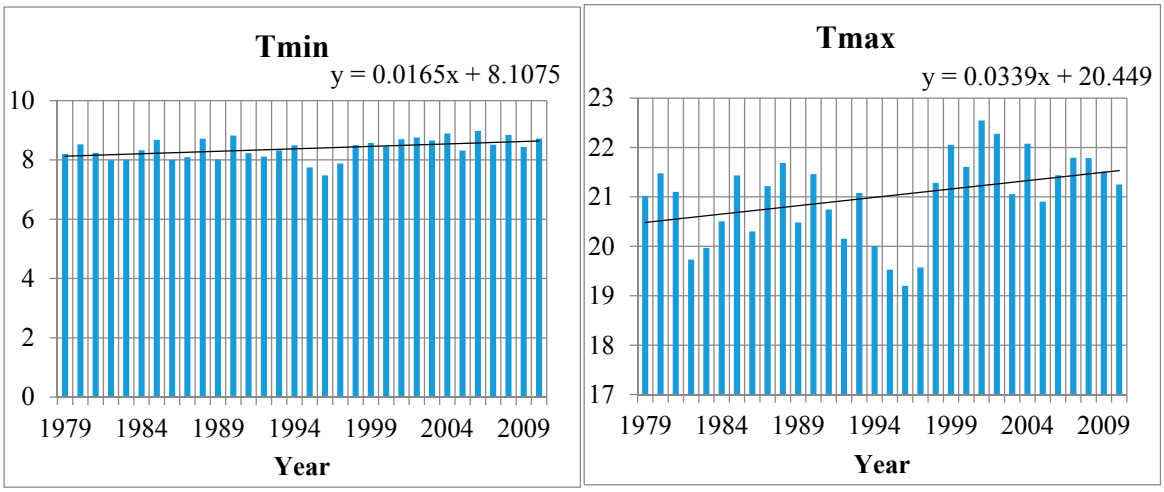

(a) (b)

Figure 4. Historical climatic trend of Mangla Watershed (a) Tmax (b) Tmin.

From figure 4 it is clear that temperature in observed period has increased over the base period. The rate of increase in Tmax and Tmin is 0.339°C and 0.165°C, respectively, per decade. The rate of increase in Tmax is more than the rate of increase in Tmin.

3.1.2. Discharge Data

The river network of the Jhelum Basin and its tributaries are shown in Figure 1. Mangla Dam is at the outlet point of the entire basin. Therefore, the watershed area of the Jhelum River Basin, which contributes the runoff to the Mangla dam was considered for the hydrological analysis. The daily discharge data from eight flow gauging stations was collected from the WAPDA, Pakistan. The data availability period along with other characteristics is presented in Table 2. The average monthly flow (1979-2010) from the different sub-basins and also from the whole Jhelum River Basin is presented in Table 3.

Preprints (www.preprints.org) | NOT PEER-REVIEWED | Posted: 24 August 2016 doi:10.20944/preprints201608.0200.v1

Peer-reviewed version available at Water 2016, 8, 389; doi:10.3390/w8090389

Table 2. Hydrological stations in the Jhelum Basin.

Sr. No.	Station	River	Latitude	Longitude	Elevation	Area	observation period
			N	E	m, MSL	Km²	
1	Naran	Kunhar	34.908	73.651	2,400	1,036	1960-2010
2	Garhi Habib Ullah/Talhatta	Kunhar	34.472	73.342	900	2,354	1960-2010
3	Muzaffar Abad	Neelum	34.367	73.469	670	7,278	1962-2010
4	Domel	Jhelum	34.367	73.467	701	14,504	1974-2010
5	Kotli	Poonch	33.489	73.885	530	3,238	1960-2010
6	Palote	Kanshi	33.222	73.432	400	1,111	1970-2010
7	Azad Pattan	Jhelum	33.73	73.603	485	26,485	1974-2010
8	Mangla	Jhelum	33.124	73.633	282	33,470	1922-2010

Table 3. Mean monthly flow (m³/s) for the period of 1979-2010.

Station Name	Jan	Feb	Mar	Apr	May	Jun	Jul	Aug	Sep	Oct	Nov	Dec	Annual (J-D)
Naran	10	8	8	21	76	142	124	68	35	21	15	12	45
Gari-habib	24	26	46	100	196	258	230	144	81	46	32	28	101
Muzafffar-Abad	64	79	179	472	780	798	630	414	227	115	83	67	326
Domel	105	183	411	616	681	519	446	367	250	136	99	101	326
Kotli	58	103	189	178	127	119	225	255	136	101	45	57	133
Polatoe	2	4	3	3	1	2	20	21	8	2	1	2	6
Azad Pattan	231	360	749	1,317	1,763	1,676	1,415	1,025	629	349	249	234	833
Mangla	308	498	998	1,551	1,929	1,833	1,728	1,378	813	482	309	309	1,011

The mean monthly flow (1979-2010) from the different tributaries and also for the whole Jhelum River Basin is presented in Table 3.

Table 4. Average monthly temperature and snow in Mangla Watershed 1981-2010.

Parameter	Jan	Feb	Mar	Apr	May	Jun	Jul	Aug	Sep	Oct	Nov	Dec
Tmax	7.8	8.8	13	19.1	24.4	28.6	28.2	27.3	26	21.3	15.5	10.2
Tmin	-2.1	-0.4	3.6	8.4	12.5	15.7	17.3	17	13.8	8.3	3	-0.4
Snowfall (mm)	60	83	76	0	0	0	0	0	0	0	9	38
Snow melt (mm)	5	6	15	23	86	99	27	0	0	0	2	3
% of Snow melt in Q	2	2	5	9	32	38	10	0	0	0	1	1

The mean monthly runoff of the Jhelum River at Mangla Dam varies between 309 and 1,929 m³/s. The minimum flow occurs in November, while the maximum flow happens in May. Variations in the temperature and precipitation pattern lead to prominent changes in the stream flows. The mean annual discharge at the Domel gauging station, Muzaffarabad and Azad Patten is 326 m³/s, 326 m³/s & 833 m³/s, respectively (Table 3). The contribution of Kanshi tributary is negligible.

Annual average Tmax, Tmin, and precipitation are 21°C, 8.7°C and 1,378mm and snowmelt contribution towards flow is 31%. Snowmelt contributes of Kunhar River is almost 55%. Snowfall is maximum in February while precipitation in the form of rainfall is maximum in July. With the increase in temperature, snow starts melting at a high rate in April and by the middle of July, most of the snow becomes part of the runoff (Table 4).

3.1.4. Spatial Data

DEM

Table 5. Hypsometric analysis of the Jhelum River Basin.

Sr. No.	Elevation (m)	Mangla	Upper Jhelum	Neelum	Kunhar	Poonch	Kanshi	Kahan
1	500	4.74	0.00	0.00	0.00	5.19	56.88	69.60
2	1,000	8.61	0.40	0.58	2.75	25.94	43.12	28.86
3	1,500	7.74	1.63	2.66	7.77	27.47		1.54
4	2,000	22.23	37.82	5.14	8.54	16.83		
5	2,500	12.75	18.14	10.25	9.67	9.96		
6	3,000	12.30	14.28	18.70	11.73	6.79		
7	3,500	11.14	10.87	21.84	14.02	3.60		
8	4,000	11.36	10.56	21.48	20.83	2.93		
9	4,500	8.08	5.61	16.72	22.56	1.28		
10	5,000	1.00	0.68	2.42	2.14	0.02		
11	5,500	0.05	0.02	0.20	0.003			
12	6,000	0.002		0.003				
13	6,218	0.004		0.002				

The Digital Elevation Model (DEM) was downloaded from NASA Shuttle Radar Topographic Mission (SRTM). The SRTM DEM has a resolution of 30 x 30 m at the equator and were delivered in mosaiced 1-arc second product pans for easy download and use. The basin and sub-basins defined mechanically from the DEM in the SWAT model. Neelam and Kunhar sub-basins are main source of snow-melt runoff in the Mangla Dam, having more than 70% area above 3,000m MSL. DEM statistics showed that maximum, minimum, mean elevation and the standard deviation is 6,276m, 261m, 3,041m and 1,581, respectively. The elevation ranges in the Jhelum sub-basins are as presented in Table 5.

Soil Data

Soil data was downloaded from the Digital Soil Map of the World (DMSW) from following website http://www.fao.org/geonetwork/srv/en/metadata.show?id=14116. DSMW vector data from FAO Soils Portal for South Asian countries was used and projected to WGS-1984 UTM Zone-43N coordinate system. Soil data is re-classified into eleven classes (Figure 4). The Dominant soil group is Gleyic Solonchak which covers 48.61% of the area of the basin. The remaining sets comprise Calcaric Phaeozems, Mollic Planosols, Haplic Chernozems, Haplic Solonetz, Calcic Chernozems, Gelic Regosols, Gleyic Solonetz, Luvic Chernozems, Lithic Leptosols and Dystric Cambisols, which occupy 22.95%, 20.24%, 1.62%, 1.51%, 1.15%, 1.09%, 1.09%, 0.71%, 0.70% and 0.35% of the area, respectively. The sand, silt, clay and rock amounts of each soil class, as well as their soil parameters, were determined by the Food and Agriculture Organization of the United Nations (FAO) digital soil images of the globe (Table 6). Soil properties like as soil bulk density, texture, soil electric conductivity, soil composition, and soil available water capacity of clay, silt and sand can be obtained

Peer-reviewed version available at Water 2016, 8, 389; doi:10.3390/w8090389

from the dataset [29]. The soil data set can be found in polygon or in a grid format. A major portion of the soil is loam that is why silt and clay are in the main proportions in river water.

Table 6. Soil constituents and parameters in Mangla River Basin.

Soil Type	Percentage of Basin Area (%)	Texture	Soil Bulk Density (g/cm3)	Hydrologic Group	Soil available water capacity (mm/mm)	Hydraulic conductivity (mm/h)	Composition (%)			Soil electric conductivity (ds/m)
							Sand	Silt	Clay	
Gelic Regosols	1.1	Silt loam	1.47	B	150	0.02	26	63	11	0.1
Gleyic Solonetz	1.1	Loam	1.36	B	150	0.02	32	43	25	1.6
Calcaric Phaeozems	22.9	Loam	1.38	B	150	0.02	35	43	22	0.2
Calcic Chernozems	1.1	Silty clay	1.24	B	150	0.01	13	42	45	0.2
Luvic Chernozems	0.7	Clay (light)	1.25	C	150	0.05	19	37	44	0.5
Mollic Planosols	20.2	Silt loam	1.35	B	150	0.02	24	52	24	0.1
Gleyic Solonchaks	48.6	Loam	1.39	C	150	0.07	37	42	21	8.7
Haplic Solonetz	1.5	Loam	1.39	B	150	0.02	47	29	24	0.1
Haplic Chernozems	1.6	Silt loam	1.35	B	150	0.02	23	54	23	0.1
Dystric Cambisols	0.4	Loam	1.41	B	100	0.02	42	38	20	0.1
Lithic Leptosols	0.7	Loam	1.38	B	150	0.02	42	34	24	0.1

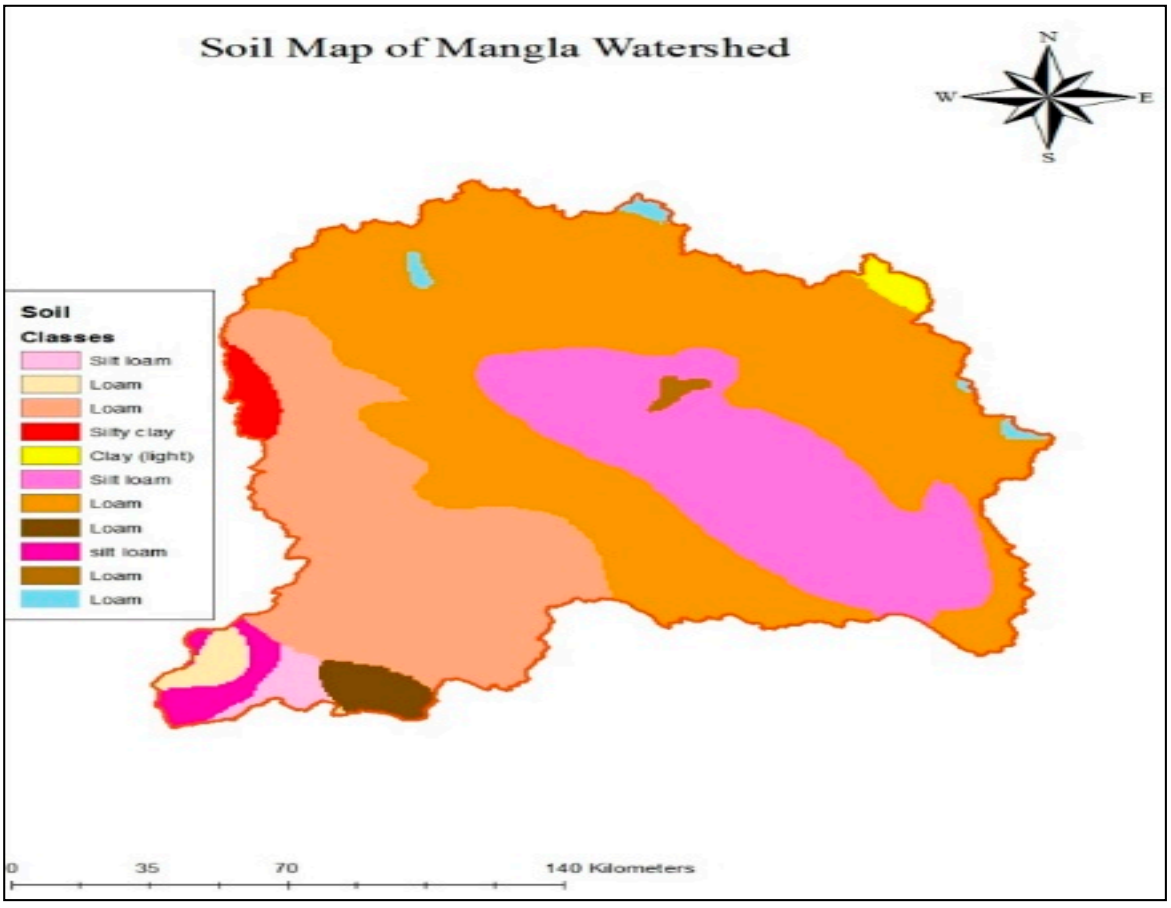

Figure 5. Soil map of the study area.

Landuse Data

The MODIS supply global maps of land cover with 500 x 500m spatial resolution. The latest version of the MODIS product is MCD12Q1 which is available on the following website (ftp://ftp.glcf.umd.edu/glcf/Global_LNDCVR/UMD_TILES/Version_5.1/2001.01.01/). There are diffrerent land cover types in the Jhelum Basin. The principal land use in the Mangla watershed is agriculture, which occupies 30.5% of the region. The remaining watershed is covered by grassland (27.8%), forest (19%), savannas (5.8%), shrubland (5.3%), barren land (2.5%), snow and ice (1.2%), water (0.6%), urban land (0.5%), and wetland (0.2).

3.2. Future climate data

The future climate data were downloaded from the following website http://climate4impact.eu/impactportal/data/advancedsearch.jsp.

Table 7. GCMs' used for climate projection in the study area.

Model	Name	Country	Emission Scenarios RCPs	Spatial Resolution
BCC-CSM 1.1-m	Beijing Climate Center (BCC), China Meteorological Administration Model	China	4.5 and 8.5	1.9° x 1.9°
CCSM4	Community Climate System Model (CCSM) National Center for Atmospheric Research (NCAR)	USA	4.5 and 8.5	0.94°x1.25°
CSIRO BOM ACCESS1-0	Commonwealth Scientific and Industrial Research Organization, Bureau of Meteorology, Australian Community Climate and Earth-System Simulator, version 1.0	Australia	4.5 and 8.5	1.9° x 1.9°
GFDL-CM3	Geophysical Fluid Dynamics Laboratory Climate Model, version 3	USA	4.5 and 8.5	2.5° x 2.0°
MIROC5	Model for Interdisciplinary Research on Climate version 5	Japan	4.5 and 8.5	1.41°x1.41°
MRI-CGCM3	Meteorological Research Institute Coupled General Circulation Model, version 3	Canada	4.5 and 8.5	1.9° x 1.9°
UKMO-HadGEM2	United Kingdom Meteorological Office Hadley Centre Global Environmental Model version 2	UK	4.5 and 8.5	2.80°x2.80°

Seven GCMs' under two scenarios from CMIP5 were considered for this study. These GCMs' cover diverse resolutions, varying from 0.94°×1.25° to 2.8°×2.8°, come from different climate centers all around the world and updated beyond the year 2000 [34]. The data for these GCMs', for selected RCPs', were downloaded for Tmax, Tmin, and precipitation. The Tmax, Tmin and precipitations used are from seven GCMs' under two RCPs'. The forcing intensities of these two RCPs' are 4.5 W/m^2 and 8.5 W/m^2, respectively, and approximately conforming to the medium and high condition. These GCMs' used for climate projection in the study area are presented in Table 7. These GCMs' cover the period from 1979 to 2100, which is divided into observed (1979-2010) and future three-time horizons (the 2020s': 2011–2040, 2050s': 2041–2070 and 2080s': 2071–2100).

4. Methodology

4.1. Downscaling and climate change analysis

Linear scaling (LS) aims to perfectly match the monthly average of corrected values with observed ones [35-37]. The monthly corrected values constructed upon the differences between observed and raw GCMs' data. The temperature is typically corrected with an additive and precipitation is typically corrected with a multiplier on a monthly basis. Monthly differences of the climate data, are obtained using observed period (1981–2010) of raw GCMs' and observed data. Following equation 1-4 are applied to correct GCMs' future precipitation and temperature data.

$$Delta\ Temperature_{30\ years} = T_{(observed,monthly)} - T_{(GCM,observed,monthly)}\ , \quad (1)$$

$$Delta\ Precipitation_{30\ years} = \frac{P_{(observed,monthly)}}{P_{(GCM,observed,monthly)}}\ , \quad (2)$$

$$T_{future,daily} = Delta\ Temperature_{30\ years} + T_{GCM,daily,future}\ , \quad (3)$$

$$P_{future,daily} = (Delta\ Precipitation_{30\ years}) \times P_{GCM,daily,future}\ , \quad (4)$$

Then climate data were analyzed relative to baseline climate on the annual and seasonal basis for future horizons.

4.2. The SWAT Model description

SWAT is used to simulate the flow of very small to very large watershed not only in the US but also in the whole world. [38-41]. SWAT can simulate the flow process in a broad range of watersheds [40,42,43]. The SWAT hydrological model was established and has been used by Hydro-Quebec for twenty years. It is presently used for forecasting of inflows on all ranges of the watershed.

The aforementioned studies showed that SWAT can work efficiently for the simulation of hydrological studies. Following conclusion has been drawn, which are also on the basis of previous studies:

i. The efficiency of the SWAT model is very high for the hydrological studies for the large catchment.
ii. Satisfactory simulation for daily, monthly, seasonally and annual runoffs'.
iii. The performance of the snow-melting process of SWAT is satisfactory.
iv. Projection of streamflows under climate change is possible.
v. SWAT is in the public domain.

Hydrologic Response Unit (HRU) is based on unique land use, soil, and the slope is the smallest unit that SWAT generates. Each HRU simulates discharge separately and then routed to obtain the total discharge from the watershed. Bearing in mind the variation in elevation in the Mangla watershed, each sub-basin was divided into elevation bands. This would imply a better analysis of snowfall and snowmelt in the basin. SWAT allows splitting each sub-basin into a maximum of 10 elevation bands. With the elevation bands, precipitation, Tmax and Tmin are calculated separately for each band. For the ET Hargreaves evapotranspiration method is used because future data of solar radiation, wind speed, and relative humidity was not available.

The hydrology constituents of the model described as follows [44]: The hydrologic replication in SWAT is made on the water balance Equation:

$$SW_t = SW + \sum(Rday - Qi - Ea - Pi - QRi)\ , \quad (5)$$

SW, soil water content
t, time
R_{day}, amount of precipitation
Q_i, amount of surface runoff
E_a, amount of evapotranspiration
P_i, amount of percolation

QR_i, amount of return flow

Detailed explanations for each parameter of the water balance equation is fully described by Arnold et al. (1998) [44].

4.2.1. Model Calibration and validation

The ArcSWAT for ArcGIS 10.2.1 interface for SWAT 2012 is used in this study to set up the model to simulate the discharge at the outlet of the Jhelum River Basin at Mangla Dam. To measure the impact of the climate change, the SWAT model was used to simulate daily stream flow over its sub-basins and then to the entire basin. This approach has been used successfully [45,46]; [47,48]. By using the climatic data from different GCMs' as an input in SWAT, various streamflow series were generated. In this study, the historical record is considered from 1981-2010 and the effect of climate change on discharge is projected from 2011 to 2100. Data of observed flow is used for calibration and validation of the model.

Calibration of a model is a procedure in which the model parameters are adjusted in such a manner that the simulated flow captures the discrepancies of the observed flow [49]. Calibration is achieved by SWAT calibration and uncertainty programs SWAT-CUP using 5000 iterations and manual calibration to achieve better agreement between simulated and observed values. Hydrological simulations were applied for each of the climate sequences. Measured discharge data of the Jhelum River basin are collected from 1981 to 2010 at all hydrological stations, data from 1986 to 1995 is used for calibration and 1996 to 2005 data is used for validation including two years as a warmup period (1979-1980).

4.2.2. Performance evaluation

Three performance evaluation parameters are used to check the performance of SWAT to project flow, namely: the coefficient of determination (R^2), Nash-Sutcliffe efficiency (NSE), and Percent Bias (PBIAS). R^2 describe the degree of collinearity between simulated and measured data, means that the proportion of the variance. R^2 ranges from 0 to 1, with higher values indicating less error variance, and typically values greater than 0.5 are considered acceptable. NSE displays how fine the observed plot fits the simulated plot. NSE ranges from 0 to 1, with higher values indicating a less error, and typically values greater than 0.5 are considered acceptable. PBIAS measures the average tendency of the simulated data to be larger or smaller than their observed counterparts, in other words, it characterizes the percent mean deviation between observed and simulated flows. PBIAS can be positive or negative, positive means underestimation and negative means overestimation, typical values –15%<PBIAS<+15 % are considered acceptable [50]. Moreover, simulated and observed data are compared graphically to discover how fine simulated flow captures the low and high observed flows.

$$R^2 = \left(\frac{\sum(X_i - X_{avg})(Y_i - Y_{avg})^2}{\sum(X_i - X_{avg})^2 \sum(Y_i - Y_{avg})^2}\right), \quad (6)$$

$$NSE = 1 - \frac{\sum(X_i - Y_i)^2}{\sum(X_i - X_{avg})^2}, \quad (7)$$

$$\text{PBIAS} = 100\left(\frac{\sum Y_i - \sum X_i}{\sum X_i}\right), \quad (8)$$

Xi, measured value

Xavg, average measured value

Yi, simulated value

Yavg, average simulated

4.3. Impact of climate change on discharge

Hydrological simulations were applied for each of the climate sequences [34]. The impact of climate change on the average annual and seasonal discharge was analyzed relative to baseline flows. Furthermore, the impact of extreme events on flows were analyzed, including flood and drought conditions. Moreover, the impact of climate change on discharge under diverse climatic scenarios

Preprints (www.preprints.org) | NOT PEER-REVIEWED | Posted: 24 August 2016 doi:10.20944/preprints201608.0200.v1

Peer-reviewed version available at Water 2016, 8, 389; doi:10.3390/w8090389

were analyzed. Finally, the impact of weather parameters on flows was estimated and two equations were developed for watershed.

5. Results and discussion

5.1 Climate Change

5.1.1. Annual

Figure 6 displays the yearly deltas of temperature and precipitation at each progressive horizon, compared to the observed period. The scatter plot shows the changes in average annual temperature as a function of the changes in average annual precipitation forecasted by each GCM.

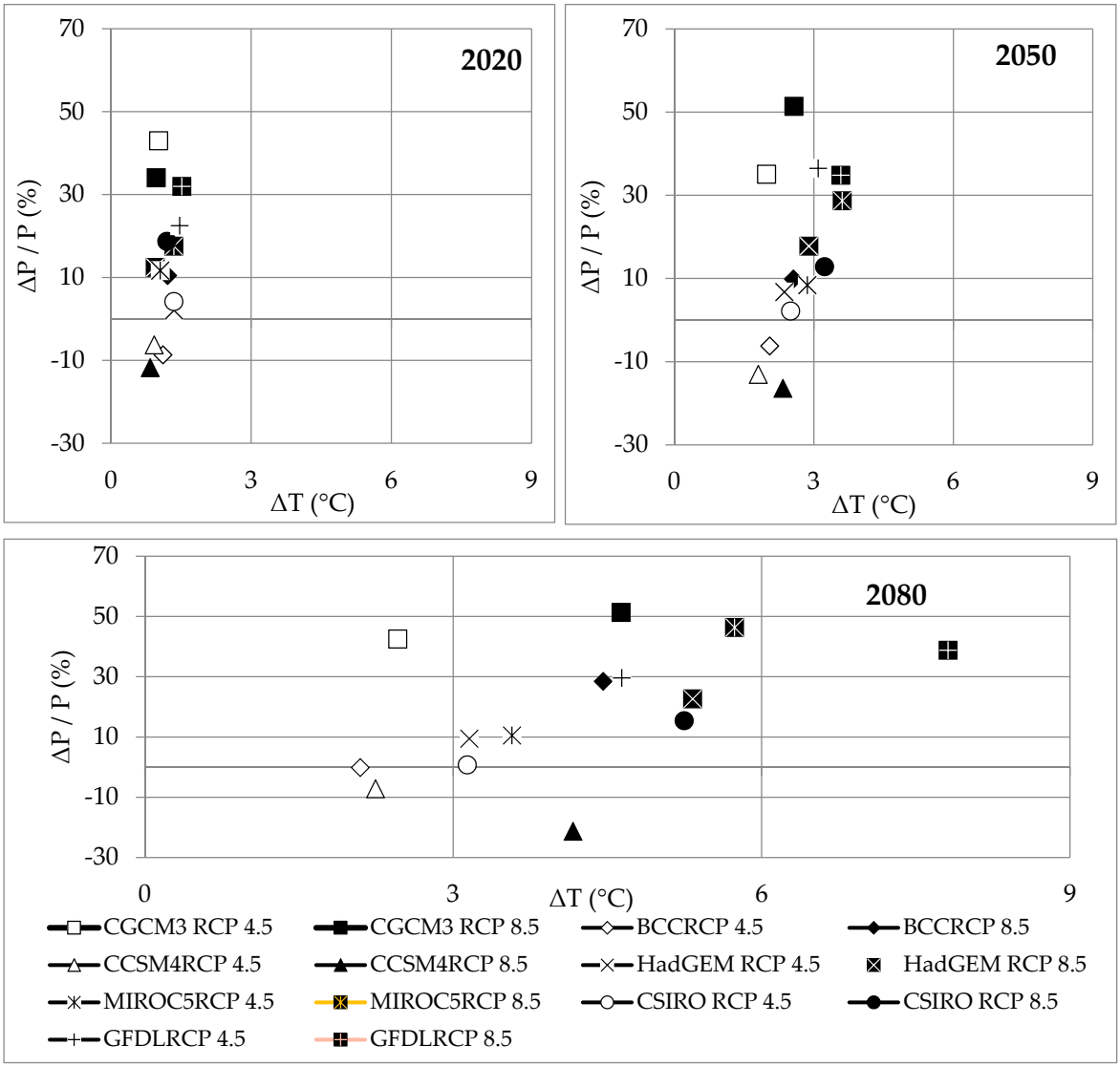

Figure 6. Annual Delta's of climate change projections.

Under RCP 4.5, change in average annual temperature and precipitation is projected in three horizons' the 2020s', 2050s' and 2080s' may vary from 0.92 to 1.47°C, -8.65 to 43%, 1.80 to 3.09°C, -13 to 37% and 2.09 to 4.64°C, -7.18 to 43%, respectively, by using seven GCMs'. Under RCP 8.5, projected change in average annual temperature and precipitation in horizon the 2020s', 2050s' and 2080s' may vary from 0.84 to 1.52°C, -12 to 34%, 2.33 to 3.61°C, -16 to 51% and 4.17 to 7.81°C, -21 to 51%, respectively, by using seven GCMs'. RCP 8.5 covered a wide range of uncertainties while RCP 4.5 covered a short range of possibilities in projected temperature and precipitation.

The annual tendency of the GCMs' is bi-vocal: five of GCMs' (CSIRO BOM ACCESS1-0, GFDL-CM3, MIROC5, MRI-CGCM3, and UKMO-HadGEM2) projected a rise in annual temperature and precipitation while two GCMs' (BCC-CSM 1.1-m and CCSM4) projected a rise in temperature but a decline in precipitation. This means that in the future a wide range of uncertainties is possible in precipitation, which is the major influencing parameter on flows. The magnitude of temperature increase is accentuated with time. While the range of precipitation variations increased over the horizons'.

5.1.2. Seasonal

There are four seasons in watershed namely, winter, spring, summer, and autumn. Observed (1981-2010) Tmax, Tmin and PPT in winter 10.9°C, 0.3°C, 370mm, spring 20.8°C, 8.4°C, 438mm, summer 29.5°C, 17°C, 406 and autumn 22.7°C, 9.1°C, 160mm are respectively.

Table 8. Projected change in mean annual and seasonal Tmax, Tmin, and PPT in three-time slices.

Winter (DJF) December, January, February, Spring (MAM) March, April, May, Summer (JJA) June, July, August, Autumn (SON) September, October, November

Sr. No.	GCM	Period	RCP	Average Increase Tmax (°C)					Average Increase Tmin (°C)					Change in PPT (%)				
				DJF	MAM	JJA	SON	Annual	DJF	MAM	JJA	SON	Annual	DJF	MAM	JJA	SON	Annual
1	MRI-CGCM3	2011-2040	4.5	0.7	0.6	0.5	0.2	0.5	2.0	1.6	1.3	1.3	1.5	7	13	95	70	43
2	BCC-CSM 1.1-m	2011-2040	4.5	1.6	0.9	1.2	1.2	1.2	1.4	0.7	0.8	1.1	1.0	-14	-1	-11	-10	-9
3	CCSM4	2011-2040	4.5	0.9	1.5	0.6	0.9	0.9	0.7	1.2	0.9	0.9	0.9	-10	-17	1	13	-6
4	UKMO-HadGEM	2011-2040	4.5	2.1	1.5	0.9	1.5	1.5	1.5	1.6	0.9	0.8	1.2	-33	48	-18	12	2
5	MIROC5	2011-2040	4.5	0.4	1.4	0.9	1.1	1.0	0.6	1.5	1.5	1.1	1.1	2	-6	50	-18	12
6	CSIRO BOM ACCESS1	2011-2040	4.5	1.8	1.3	0.5	1.3	1.2	2.0	1.5	1.1	1.3	1.5	7	11	3	-18	4
7	GFDL-CM3	2011-2040	4.5	1.8	1.5	1.3	1.8	1.6	1.2	1.1	1.5	1.5	1.3	-19	-3	44	128	23
8	MRI-CGCM3	2011-2040	8.5	0.6	0.4	0.5	0.0	0.4	2.0	1.4	1.4	1.4	1.6	-5	10	92	38	34
9	BCC-CSM 1.1-m	2011-2040	8.5	1.5	1.4	1.0	1.4	1.3	1.6	1.0	0.7	1.2	1.1	11	3	10	32	10
10	CCSM4	2011-2040	8.5	1.2	1.4	0.9	0.9	1.1	0.5	0.9	0.6	0.4	0.6	-30	-1	-2	-26	-12
11	UKMO-HadGEM	2011-2040	8.5	1.1	0.7	0.5	0.8	0.8	1.2	1.2	0.9	1.2	1.1	-24	63	-12	21	12
12	MIROC5	2011-2040	8.5	0.7	1.4	1.3	1.0	1.1	1.2	1.9	1.9	1.4	1.6	14	5	19	55	18
13	CSIRO BOM ACCESS1	2011-2040	8.5	1.1	1.4	0.5	1.4	1.1	1.2	1.6	1.0	1.3	1.3	29	28	5	6	19
14	GFDL-CM3	2011-2040	8.5	2.1	1.3	1.2	1.4	1.5	1.9	1.1	1.8	1.4	1.5	-7	-5	47	180	32
15	MRI-CGCM3	2041-2070	4.5	1.3	2.1	1.7	1.0	1.5	2.9	2.6	2.2	2.2	2.5	23	-15	85	66	35
16	BCC-CSM 1.1-m	2041-2070	4.5	3.0	3.1	1.6	1.6	2.3	2.5	2.2	1.1	1.4	1.8	-11	-18	3	14	-6
17	CCSM4	2041-2070	4.5	2.2	2.4	1.5	1.7	2.0	1.5	2.0	1.5	1.6	1.6	-45	-24	14	19	-13
18	UKMO-HadGEM	2041-2070	4.5	3.1	2.7	1.3	3.0	2.5	2.6	2.5	2.0	1.7	2.2	-21	47	-2	-15	7
19	MIROC5	2041-2070	4.5	2.6	4.0	3.1	2.2	3.0	2.5	3.4	3.2	1.8	2.7	-5	-14	46	2	8
20	CSIRO BOM ACCESS1	2041-2070	4.5	2.8	2.8	1.7	2.6	2.5	3.1	2.7	2.0	2.1	2.5	8	7	4	-28	2
21	GFDL-CM3	2041-2070	4.5	3.1	3.1	2.8	3.8	3.2	2.5	2.6	3.2	3.6	3.0	-6	-3	60	179	36
22	MRI-CGCM3	2041-2070	8.5	1.9	2.2	2.1	1.4	1.9	3.7	3.3	3.0	3.0	3.2	18	8	116	76	51
23	BCC-CSM 1.1-m	2041-2070	8.5	3.1	3.1	2.9	2.2	2.8	2.9	2.2	1.9	2.2	2.3	7	0	-3	78	10
24	CCSM4	2041-2070	8.5	2.8	3.3	2.5	2.4	2.7	1.9	2.3	1.8	1.7	1.9	-22	-33	6	-17	-16
25	UKMO-HadGEM	2041-2070	8.5	2.9	3.1	2.1	2.8	2.7	3.3	3.1	2.7	3.1	3.1	-13	59	3	16	18
26	MIROC5	2041-2070	8.5	3.1	4.3	3.3	2.8	3.4	3.4	4.5	4.4	3.0	3.8	4	5	56	78	29
27	CSIRO BOM ACCESS1	2041-2070	8.5	3.2	3.6	2.4	3.9	3.3	3.5	3.7	2.7	2.7	3.2	26	18	4	-6	13
28	GFDL-CM3	2041-2070	8.5	4.3	4.0	4.2	5.1	4.4	2.5	2.4	2.8	3.3	2.7	-15	2	59	174	35
29	MRI-CGCM3	2071-2100	4.5	1.9	2.0	2.0	1.9	1.9	3.5	2.9	2.7	2.8	3.0	10	25	81	65	43
30	BCC-CSM 1.1-m	2071-2100	4.5	2.9	2.4	1.9	2.1	2.3	2.5	1.7	1.5	1.8	1.9	-1	-8	8	5	0
31	CCSM4	2071-2100	4.5	2.6	2.9	2.1	2.5	2.5	2.0	2.3	1.8	1.8	2.0	-10	-21	2	12	-7
32	UKMO-HadGEM	2071-2100	4.5	3.8	3.6	2.3	3.5	3.3	3.4	3.2	2.7	2.7	3.0	-24	51	-3	8	9
33	MIROC5	2071-2100	4.5	3.7	4.3	3.9	2.8	3.7	3.6	3.9	4.0	2.4	3.5	-12	-4	47	8	11
34	CSIRO BOM ACCESS1	2071-2100	4.5	3.1	3.7	2.7	3.8	3.3	3.4	3.4	2.5	2.5	2.9	16	1	0	-34	1
35	GFDL-CM3	2071-2100	4.5	5.3	4.9	4.6	5.3	5.0	4.2	3.9	4.5	4.4	4.3	-16	-15	80	126	30
36	MRI-CGCM3	2071-2100	8.5	4.1	4.1	3.8	3.9	4.0	6.4	5.0	4.8	5.0	5.3	27	24	100	56	51
37	BCC-CSM 1.1-m	2071-2100	8.5	5.0	5.8	4.1	4.3	4.8	4.7	4.4	3.2	4.2	4.1	28	8	28	87	28
38	CCSM4	2071-2100	8.5	4.8	5.6	4.4	4.5	4.8	3.5	4.0	3.2	3.3	3.5	-23	-37	-6	-15	-21
39	UKMO-HadGEM	2071-2100	8.5	5.6	6.2	3.4	5.6	5.2	5.7	5.8	4.6	5.6	5.5	-11	50	28	11	23
40	MIROC5	2071-2100	8.5	5.7	6.6	5.1	4.3	5.4	5.9	6.8	6.6	4.9	6.0	1	10	92	127	46
41	CSIRO BOM ACCESS1	2071-2100	8.5	5.8	5.9	4.0	5.5	5.3	5.9	5.8	4.5	4.5	5.2	10	22	22	-5	15
42	GFDL-CM3	2071-2100	8.5	8.1	7.9	8.3	8.9	8.3	6.8	6.5	7.9	8.2	7.3	-28	-9	105	148	39

Table 8 displays the seasonal deltas of temperature and precipitation at each progressive horizon, compared to the observed period using seven GCMs' under two RCPs'. The change in average seasonal precipitation is less in winter and spring while change is precipitation is more for

summer and autumn using seven GCMs'. Monsoon rainfall is projected to be a more intense while, in winter less amount of snowfall expected due to projected increase in temperature.

There is a continuous rise in projected Tmax and Tmin in all seasons. The large increase in temperature is expected in the winter. For horizon 2080s', the autumn temperatures could increase by 8.9°C under GFDL RCP 8.5. Average seasonal change in Tmax, Tmin, and precipitation is projected to vary from 0.2 to 5.3°C, 0.6 to 2.0°C and -45.1 to 128.4%, respectively, by using seven GCMs' under RCP 4.5. While under RCP 8.5 Tmax, Tmin, and precipitation are projected to vary from 0 to 8.9°C, 0.4 to 8.2°C and -37.3 to 180.3%, respectively. RCP 8.5 covered a wide range of uncertainties while RCP 4.5 covered a short range of possibilities in projected temperature and precipitation.

5.2 Model calibration and validation

Table 9. Model parameters used to calibrate discharge.

Sr. No.	Parameter	Description and unit	Initial Range	Final parameter
1	SOL_AWC	Available water capacity of the soil layer (mmmm−1 soil)	0 - 1	0.04
2	ALPHA_BF	Base flow alpha factor (days) (–)	0 - 1	0.048
3	SFTMP	Snowfall temperature (°C)	-20 - 20	-0.78
4	SMTMP	Snow melt base temperature (°C)	-20 - 20	2.43
5	SMFMX	Maximum melt rate for snow during year (occurs on summer solstice) (–)	0 - 20	2.98
6	SMFMN	Minimum melt rate for snow during the year (occurs on winter solstice) (–)	0 - 20	1.57
7	TIMP	Snow pack temperature lag factor (–)	0 - 1	0.94
8	SNOCOVMX	Minimum snow water content that corresponds to 100% snow cover (–)	0 - 500	48
9	SNO50COV	Snow water equivalent that corresponds to 50% snow cover (–)	0 - 1	0.43
10	ESCO	Soil evaporation compensation factor (–)	0 - 1	0
11	EPCO	Plant uptake compensation factor (–)	0 - 1	0.97
12	SOL_K	Saturated hydraulic conductivity (mmh−1)	0 - 2000	1.45
13	CH_K2	Effective hydraulic conductivity in the main channel alluvium (mmh−1)	0.001 - 500	0.001
14	GW_DELAY	Groundwater delay (days)	0 - 500	31
15	GWQMN	Threshold depth of water in the shallow aquifer required for return flow to occur (mm)	0 - 5000	0
16	RCHRG_DP	Deep aquifer percolation fraction (–)	0 - 1	0.9
17	GW_REVAP	Groundwater "revap" oefficient	.02-.2	.02
18	REVAPMN	Threshold depth of water in the shallow aquifer for "revap" to occur (mm)	0 - 500	500
19	CH_N2	Manning's "n" value for the main channel (–)	-0.01 - 0.3	0.014

For sensitivity analysis, twenty-seven parameters were considered out of which nineteen were found relatively sensitive. Preceding studies were the point of focus for calibration to get sensitive parameters [42,51-54] (Figure 2). Among the sensitive parameters, snow parameters (SMFMX, SMFMN, SFTMP, SMTMP, TIMP, SNO50COV and SNOCOVMX) were found more sensitive for Neelam and Kunhar sub-basins as these basins are mainly snow-fed, while for Poonch, Kanshi, Lower Jhelum and Kahan sub-basins other parameters (ALPHA_BF, GW_REVAP, REVAPMN, GW_DELAY, GWQMN, RCHRG_DP, SOL_K, SOL_AWC, ESCO, EPCO, and CH_N2) were found more sensitive. A brief description of each parameter is mentioned in the SWAT user's manual [55].

Preprints (www.preprints.org) | NOT PEER-REVIEWED | Posted: 24 August 2016 doi:10.20944/preprints201608.0200.v1

Peer-reviewed version available at Water 2016, 8, 389; doi:10.3390/w8090389

The optimum value of each parameter is given in Table 9 and sensitivity rank of each parameter is given in Figure 7.

The t-test offers a measure of sensitivity, the largest absolute value represents higher sensitivity and p-value determined the significance of sensitivity. A value close to zero has more significance. Sensitivity rank in reverse order is shown in figure 7. Rank of parameters increase from bottom to top as p-value is close to 0 and t-value is very high at the bottom of figure 7. SNOCOVMX is the least important parameter because of the very high p-value and very low t-value. While CH_N2 is most important influencing parameter on flow as very low p-value and very high t-value.

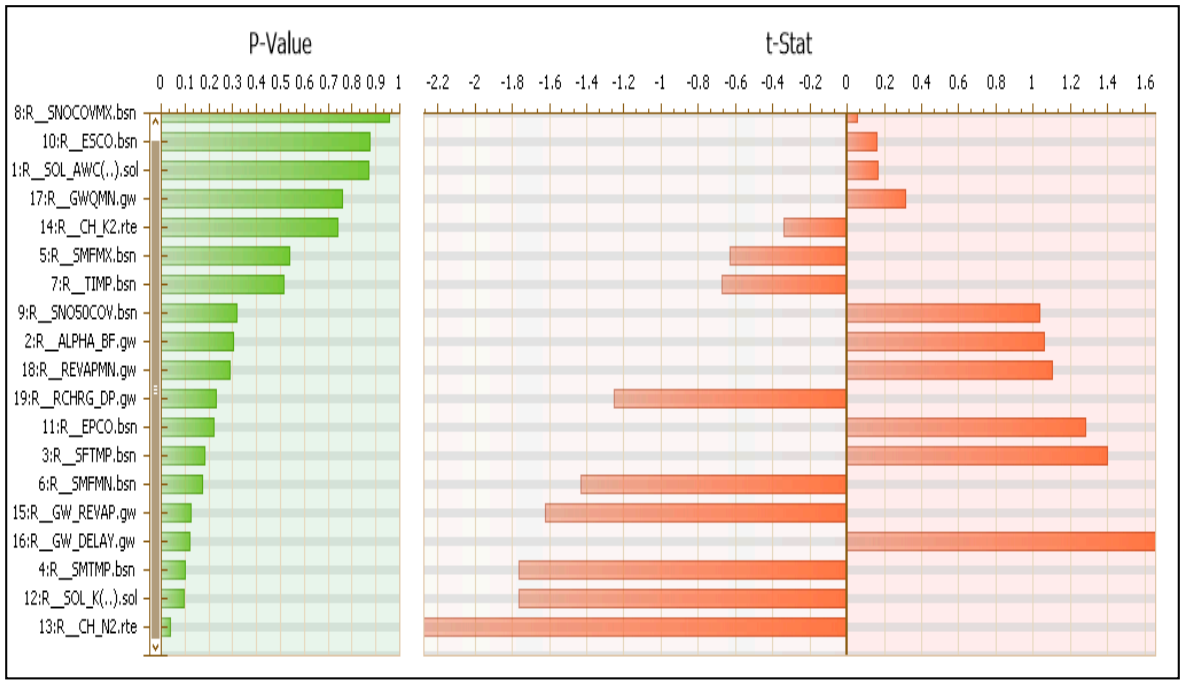

Figure 7. Sensitivity analysis of parameters using SWAT-CUP.

Table 10. Statistical analysis for calibration.

Sr. No.	Name	Calibration (1986-1995)		
		R^2	NSE	PBIAS
1	Mangla Dam	0.82	0.77	-10.66
2	Azad Pattan	0.88	0.85	-1.70
3	Kohala	0.88	0.85	-1.13
4	Domel	0.69	0.68	-4.38
5	Muzaffar Abad	0.83	0.72	-5.46
6	Gari-Habibullah	0.75	0.60	-10.81
7	Kotli	0.66	0.62	13.81

Table 11. Statistical analysis for validation period.

Sr. No.	Name	Validation (1996-2005)		
		R^2	NSE	PBIAS
1	Mangla Dam	0.73	0.68	-10.98
2	Azad Pattan	0.82	0.81	-3.87
3	Kohala	0.83	0.81	-3.16
4	Domel	0.63	0.61	2.40
5	Muzaffar Abad	0.68	0.66	-11.33
6	Gari-Habibullah	0.65	0.55	-14.09
7	Kotli	0.64	0.60	14.52

Preprints (www.preprints.org) | NOT PEER-REVIEWED | Posted: 24 August 2016 doi:10.20944/preprints201608.0200.v1

Peer-reviewed version available at Water 2016, 8, 389; doi:10.3390/w8090389

The calibrated model parameters were applied to simulate the discharge (Table 9). Table 10 and 11 show the model's evaluation parameters (R^2, NSE, and PBIAS) calculated using the observed and simulated discharge for calibration (1986–1995) and validation (1996–2005) at different measuring stations. In the case of calibration, the values of R^2, NSE, and PBIAS ranged from 0.66 to 0.88, 0.60 to 0.85 and -10.81 to 13.81% and in the case of validation the values of R^2, NSE, and PBIAS, vary from 0.64 to 0.83, 0.55 to 0.81 and -14.09 to 14.52%. Simulated and observed discharge at Azad Pattan has R^2, NSE, and PBIAS 0.88, 0.85 and -1.70%, respectively (Table 10).

Comparison between observed and simulated flows, including precipitation for the calibration and validation are presented in Figures 8. At different measuring stations, shapes of observed flow were well captured by the shapes of the simulated flow. Nevertheless, some high peaks and low flows were not matched well. At Azad Pattan, a few peak and low flows were underestimated by the model while on other occasions a few were overestimated. This underestimation/overestimation might be due to the scarcity of precipitation gauges available in the basin.

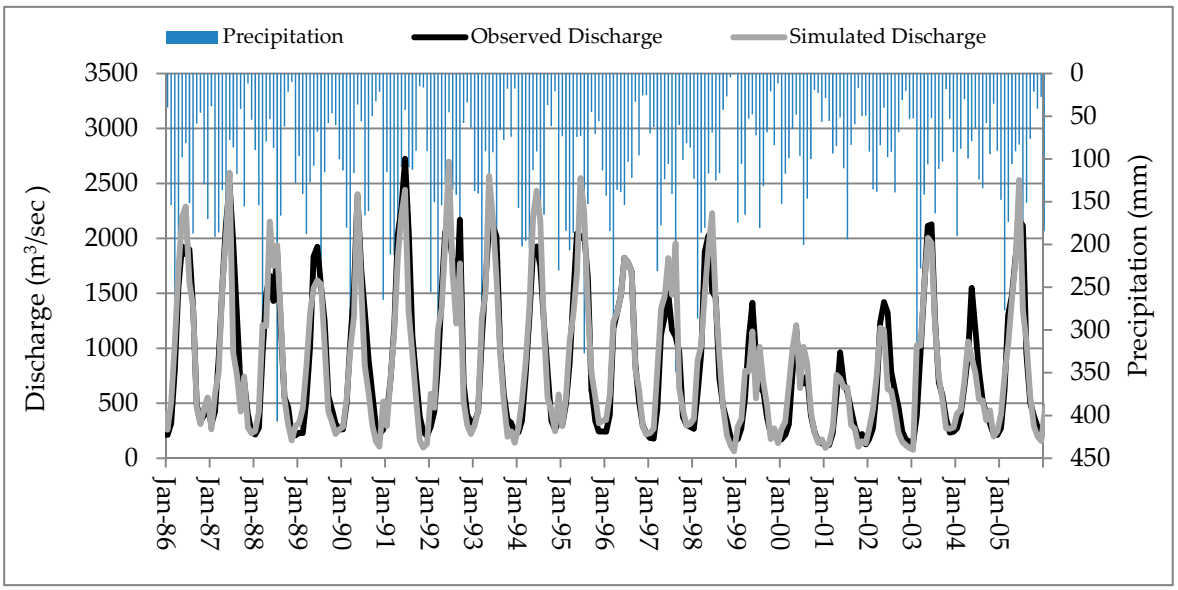

Figure 8. Comparison between observed and simulated flows at Azad-Pattan including precipitation.

5.3 Impact of climate change on discharge

5.3.1 Annual and seasonal variations

The impact of climate change on the average annual and seasonal flow is illustrated in Fig. 9. Flows are expressed as a percentage relative to observed period, for each climate projection and horizon.

Under RCP 4.5, change in average annual flow is projected in horizons' the 2020s', 2050s' and 2080s' may vary from -8.7 to 61.1%, -22.9 to 56.3% and -12.3 to 59.7%, respectively, by using seven GCMs'. Under RCP 8.5, change in average annual flows is projected in horizons' the 2020s', 2050s' and 2080s' may vary from -10.6 to 70.4%, -20.4 to 97.7% and -27.2 to 74.2%, respectively, by using seven GCMs'. RCP 8.5 covered a wide range of uncertainties while RCP 4.5 covered a short range of possibilities in projected annual flows. The annual tendency of the GCMs' is bi-vocal: six GCMs' (CSIRO BOM ACCESS1-0, GFDL-CM3, MIROC5, MRI-CGCM3, BCC-CSM 1.1-m and UKMO-HadGEM2) projected a rise in annual flows while one GCM (CCSM4) projected a decrease in flows. This means that a wide range of uncertainties in projected flows using GCMs' uder RCPs'.

There are four seasons in watershed namely; winter, spring, summer, and autumn. Observed (1981-2010) inflows in winter 367m^3/sec spring 1502m^3/sec, summer 1639m^3/sec, autumn 509m^3/sec are respectively. The change in average seasonal flows is more relative to annual variations in discharge. Variation in winter and spring discharge are mostly positive even with the decrease in precipitation while the change in flows is mostly negative for summer and autumn using seven GCMs'. This may be due to early snowmelt owing to increase in temperature. The largest increase in

Preprints (www.preprints.org) | NOT PEER-REVIEWED | Posted: 24 August 2016 doi:10.20944/preprints201608.0200.v1

Peer-reviewed version available at Water 2016, 8, 389; doi:10.3390/w8090389

flows are projeted in winter. For horizon 2080s', the winter flows could increase more than 150% under GFDL RCP 8.5. The change in average seasonal flows under RCPs' 4.5 and 8.5 are projected to be -29.1 to 130.7% and -49.4 to 171%, respectively, by using seven GCMs'. RCP 8.5 covered a wide range of uncertainties while RCP 4.5 covered a short range of possibilities in projected flows.

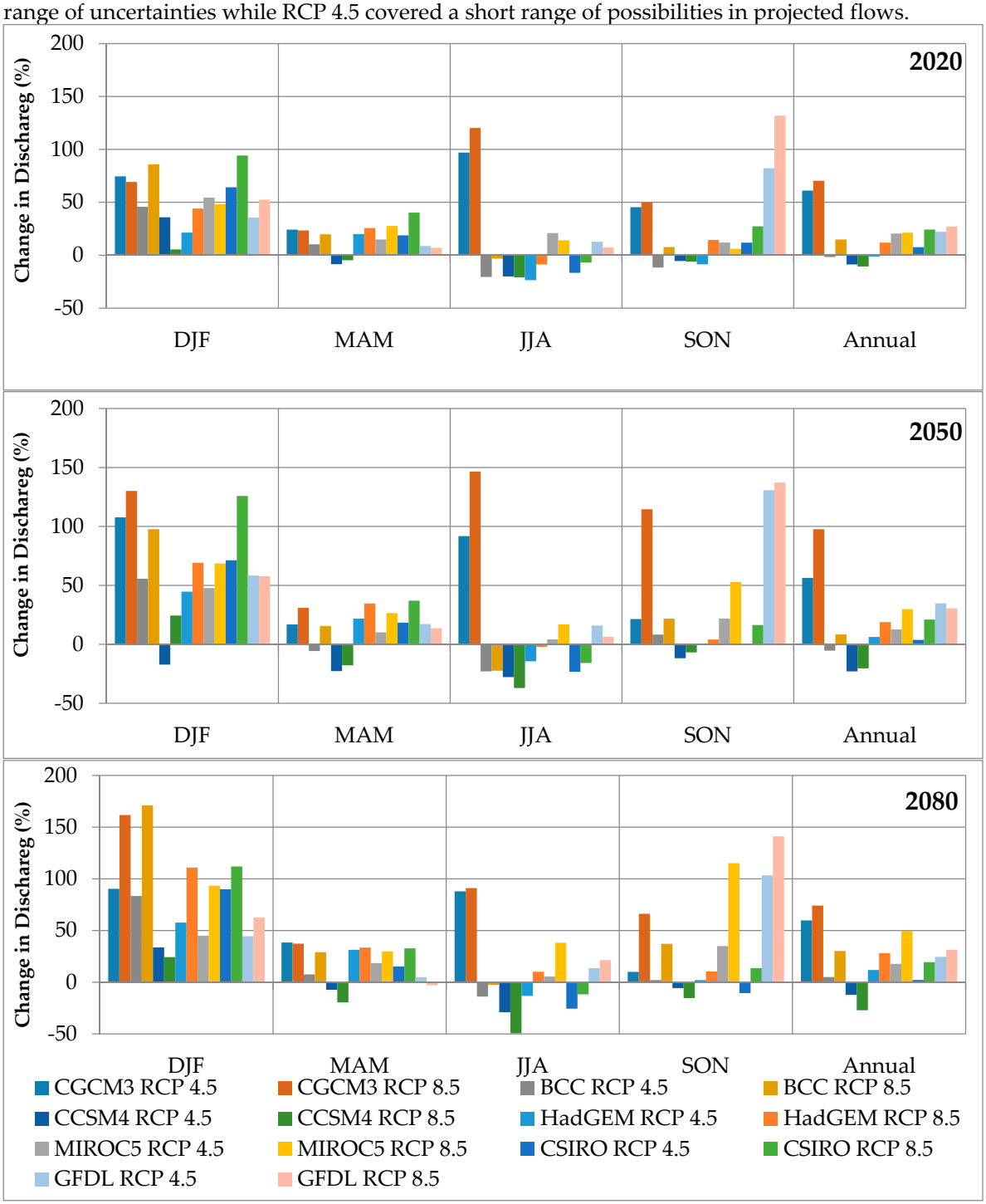

Figure 9. Mean annual and seasonal discharges, as a percentage of the annual production of the observed period.

5.3.2 Impact of extreme events on discharge

Extreme events are the complex phenomena which are characterized on the basis of frequency, duration, and intensity. The extreme precipitation events are expected to increase in future because global warming will have an impact on the frequency & intensity of extreme events [56]. Therefore, it is essential to cover all possible ranges of intensities of precipitation in 1–day, 2-Day and 3-day from 10mm/day to 600mm/day by increasing with an increment of the 10mm/day. After, calibration and validation of SWAT model, plausible user defined database were generated for extreme conditions.

Peer-reviewed version available at Water 2016, 8, 389; doi:10.3390/w8090389

The impact of extreme events on discharge was analyzed by selecting a wide range of probable 1-day, 2-day and 3-day precipitation events (Figure 10). Pakistan had suffered a lot from flood in 2010 because of the heavy monsoon rainfall [57]. One fifth of Pakistan was under water [58] and recorded precipitation in a day in Islamabad and the nearby station was 600mm/day. Heavy floods due to extreme rainfall events can generate excessive flow and sediment load that can affect Mangla Reservoir, consequently, it is essential to include the impact of extreme events on streamflows under climate change impact studies.

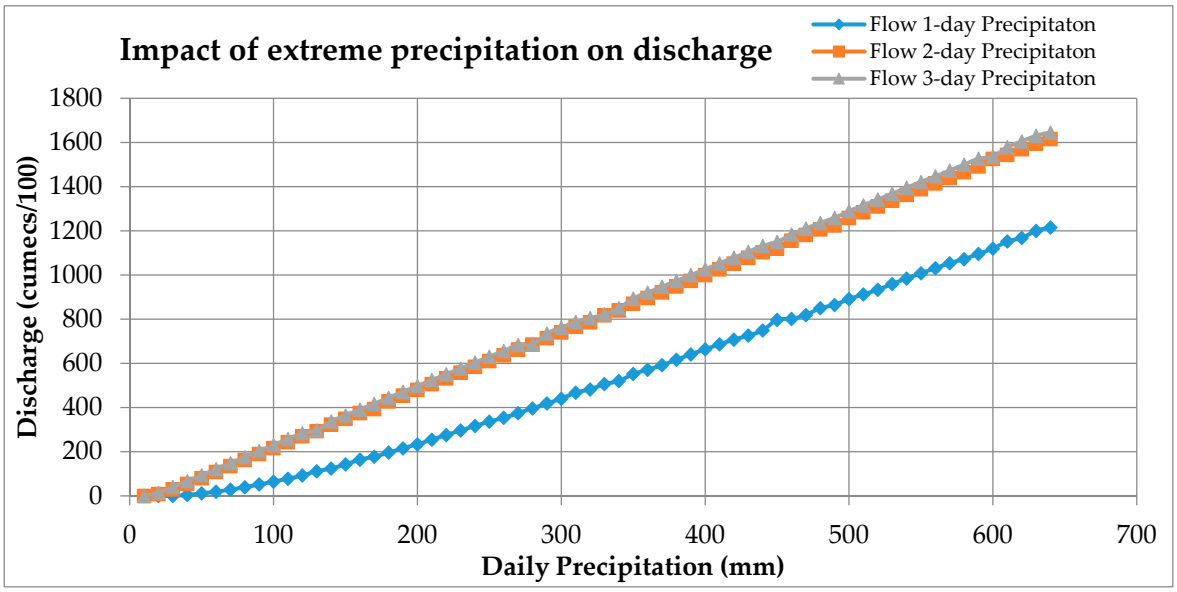

Figure 10. Impact of extreme rainfall events on discharge.

Time of concentration for Mangla watershed is 49hours at Mangla Dam. Mangla Reservoir has the capacity to discharge 30,000m³/sec. The average rainfall of 230mm/day is enough to create flooding in Mangla Reservoir; it can happen in 1-day, 2-Day or 3-day events. the amount of flood with respect to each extreme event is shown in figure 10. This graph is extremely helpful to predict flooding against each probable event of precipitation. It will be very helpful for planner and policymakers to act instantaneously after each event in Mangla watershed to operate the reservoir accordingly, to get maximum benefits from expected floods. Then flood will become an opportunity to maximize benefits or minimize loss.

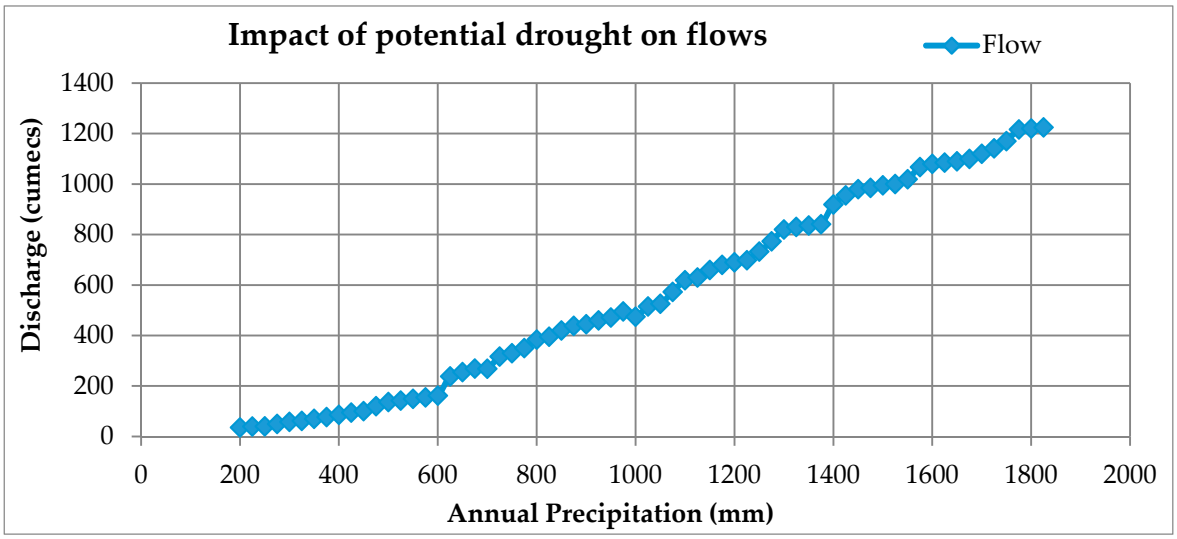

Figure 11. Impact of drought condition on discharge.

The amount of flow with respect to different annual precipitation is displayed in figure 11. During extreme drought condition, very less amount of mean annual flow is expected in the reservoir

due to less precipitation, hence opportunity to get benefits is very less but reservoir can be operated differently to deal this extreme condition. While, in wet condition more amount of flow will come in the reservoir due to increased precipitation, hence opportunity to attain benefits will be more. This graph is extremely helpful to predict flow against each probable annual precipitation from 200mm to 2000mm with an increment of 20mm/annum. It will be very helpful for planner and policymakers to act instantaneously after each event in Mangla watershed to operate the reservoir accordingly, to get maximum benefits from expected droughts. Then drought will become an opportunity to maximize benefits or minimize loss. In conclusion, the extreme event is not only a threat, but also an opportunity to get maximum benefits from the reservoir.

5.3.3 Impact of climate change on discharge under diverse climatic scenarios'

The change in mean annual (2011-2100) precipitation, Tmax, and Tmin in the watershed may from -50 to +70%, 3 to 6°C and 2.5 to 8°C, respectively, under RCPs' 4.5, and 8.5. The plausible scenarios were built to simulate the impact of these diversified conditions. Table 12 shows a change in discharge in percentage relative to the baseline period. With the only growth in precipitation by 70%, projected increase in discharge is 79% in Mangla watershed, while the combined increase in precipitation (70%), Tmax (6°C), and Tmin (8°C increase in flow will be only 68.5%. This means that with only increase in precipitation projected change in discharge is much higher than the combined increase in precipitation, Tmax, and Tmin. Furthermore, the same trend is projected under decrease in precipitation. Neelam and Kunhar Rivers are snow-fed that is why with an increase in the temperature decrease in discharge in these sub-basins is relatively less with respect to Upper Jhelum, Lower Jhelum, Kanshi, and Kunhar sub-basins. With the increase in temperature projected flows are expected to decrease. While with the increase in precipitation projected flows are projected to increase.

Table 12. Change in projected discharge in percentage under different climatic scenarios'

Climate	Mangla Watershed	Upper Jhelum	Neelum River	Kunhar River	Kanshi River	Poonch River	Lower Jhelum
Area ($km^{2)}$	33,420	14,400	7,421	2,632	1,303	4,398	2,813
P+70	79	66.5	80.3	62.6	139.5	120.2	147.2
P+70 Tmax3 Tmin2.5	74	61.8	78.7	55.2	123.2	104.9	129.1
P+70 Tmax6 Tmin8	68.5	59.2	64.4	47.1	116.1	98.1	118.8
P-50	-63	-66.1	-57.3	-67.7	-75	-69.5	-191.1
P-50 Tmax3 Tmin2.5	-65.7	-67.8	-59	-68.8	-75.6	-70.4	-60.1
P-50 Tmax6 Tmin8	-70.2	-72.1	-66.3	-73.5	-77.8	-73.3	-3.1

5.3.4 Impact of climatic parameters on flows

There are two major climatic parameters having an influence on discharge; precipitation and temperature. Generally, precipitation is the major cause of runoff, but watershed with more than 30% of snow-melt contribution in the runoff, the temperature is also important and cannot be ignored. Figure 12 shows the impact of only precipitation change on flows relative to the change in baseline precipitation. It is very clear from figure 12 that with the increase in precipitation flows are expected to increase. While, with the decrease in projected precipitation flows, are expected to decrease. The correlation between precipitation and flows is very strong (99.88%), which means that this equation is strongly predicting flows with the change in precipitation. With the change of 10% in precipitation, flows are expected to change by 10.7%. This equation is very useful for planners and policy makers to act accordingly to a wide range of possibilities.

Preprints (www.preprints.org) | NOT PEER-REVIEWED | Posted: 24 August 2016 doi:10.20944/preprints201608.0200.v1

Peer-reviewed version available at Water 2016, 8, 389; doi:10.3390/w8090389

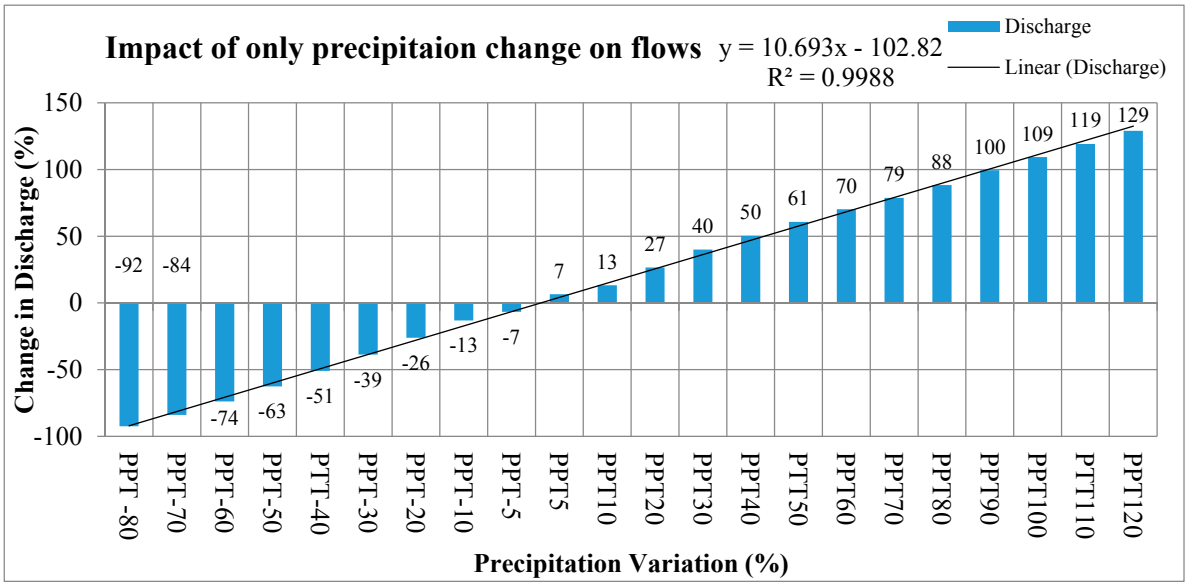

Figure 12. Impact of only precipitation changes on flows

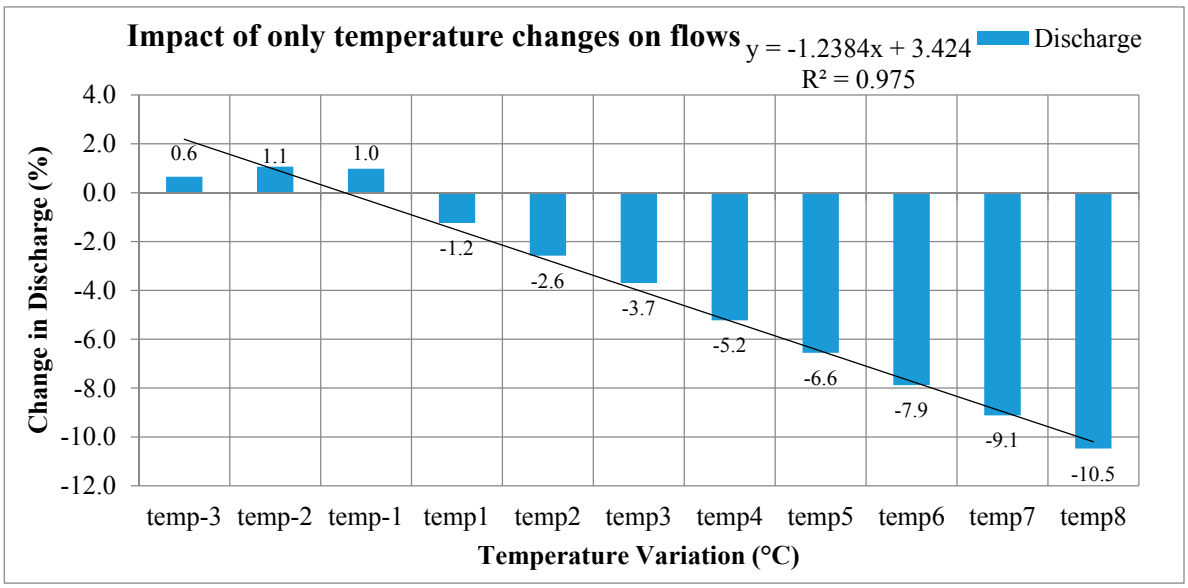

Figure 13. Impact of the only temperature changes on flows

Figure 13 shows the impact of only temperature change on flows relative to the change in baseline temperature. It is very clear from figure 13 that with the increase in temperature, flows are projected to decline. While, with the reduction in projected temperature flows, are expected to surge. The correlation between temperature and flows is very strong (97.5%), which means that this equation is strongly predicting flows with the change in temperature. With the change in 1°C of temperature, flows are expected to change by 1.24%. This equation is very useful for planners and policy makers to act accordingly to a wide range of possibilities.

Precipitation is more sensitive parameter relative to temperature to cause variation in projected flows.

6. Conclusions

This study evaluates the impact of climate change on inflows in the Mangla Basin situated in the north-eastern part of Pakistan. In this paper a multi-climate model, the multi-emission scenario is used for the assessment of climate change impact. The SWAT hydrological model is used to simulate

the changes in flows. Calibration, validation, and sensitivity analyses suggest that the SWAT model can be applied with confidence to simulate future variations in discharge under climate change.

The Tmax and Tmin are projected to increase for all three-time horizon under both RCPs' 4.5 and 8.5. The rise in Tmax is expected more than Tmin. Precipitation is projected to increase using five GCMs' while, precipitation is projected to decrease using two GCMs under both RCPs' 4.5 and 8.5. Results indicate that large uncertainties exist in all the expected future hydrological variables due to differences between the climate model and emission scenarios'. RCP 8.5 covered a wide range of uncertainties while RCP 4.5 covered a short range of possibilities in projected flows. In general, higher discharge is expected during the winter. Therefore, it is impossible to forecast future discharge accurately. Regardless of these uncertainties, it has to be noted that predictions of hydrological changes in the basin are extremely dependent on the direction of the projected changes in precipitation. Moreover, the results indicate that discrepancies between climate models and emission scenarios are noteworthy, this study also highlights the need for a multi-climate model approach as a substitute for just one climate model under one emission scenario when assessing the possible impacts of climate change.

A wide range of uncertainties is covered under extreme events impact on flows which will be very helpful for water resources managers to deal with various extremes. Two equations regarding precipitation and temperature impact on inflows to Mangla reservoir will be very useful for planners and policy makers to act accordingly to a large range of possibilities. The results of this study are useful to development planners, decision-makers, and other participants when planning and executing suitable water management policies to adapt the climate change. Finally, some of the results show very high variation in flows, which must raise alarm among the hydropower developers as these specific results must cause strategies to reevaluate the design and operation of future and existing dams.

Supplementary Materials: The following are available online at www.mdpi.com/link, Figure S1: title, Table S1: title, Video S1: title.

Acknowledgments: I would like to recognize and offer thankfulness to Pakistan Meteorological Department (PMD), Water and Power Development Authority (WAPDA) of Pakistan, India Meteorological Department (IMD), Climate Forecast System Reanalysis (CFSR), for providing the essential and valuable data for this study. Profound appreciation is extended to Higher Education Commission (HEC) of Pakistan and Asian Institute of Technology (AIT) providing monetary support to the author for his doctoral studies at AIT. I seriously admit that without HEC funding, it might be hard to finish my research study.

Author Contributions: All authors have contributed to the idea and hypothesis development, method development, analysis, interpretation of the results and writing the manuscript.

Conflicts of Interest: The authors declare no conflict of interest.

Abbreviations

The following abbreviations are used in this manuscript:

°C: Degree Centigrade
ACCESS1-0: Bureau of Meteorology, Australian Community Climate and Earth-System Simulator, version 1.0
AR5: 5th Assessment Report
ARCGIS: Aeronautical Reconnaissance Coverage Geographic Information System
BCC-CSM: Beijing Climate Center, China Meteorological Administration
CCSM4: Community Climate System Model version 4
CGCM3: Canadian Centre for Climate Modeling version 3
CIMP5: Climate Model Intercomparison Project Phase 5
CSIRO BOM: Commonwealth Scientific and Industrial Research Organization
DEM: Digital Elevation Model
DJF: December, January, February
FAO: Food and Agricultural Organization
GCMs: General Circulation Models
GFDL-CM3: Geophysical Fluid Dynamics Laboratory Climate Model version 3
GHGES: Greenhouse Gas Emission Scenarios

GIS: Geographical Information System
HEC-ResSim: Hydrologic Engineering Center Reservoir System Simulation
HPP: Hydropower potential
HRU: Hydrologic Response Unit
IMD: Indian Metrological Department
IPCC: Intergovernmental Panel on Climate Change
JJA: June, July, August
km^2: Square Kilometers
km^3: Cubic Kilometers
LULC: Landuse Land Cover
m: Meter
m^2: Square Meters
m^3: Cubic Meters
MAM: March, April, May
MIROC5: Model for Interdisciplinary Research on Climate version 5
mm: Millimeter
MODIS: Moderate Resolution Imaging Spectrometer
MRI-CGCM3: Meteorological Research Institute Coupled General Circulation Model, version 3
MSL: Mean Sea Level
MW: Mega Watts
NSE: Nash-Sutcliffe Efficiency
PMD: Pakistan Metrological Department
RCP: Representative Concentration Pathway
SON: September, October, November
SRES: Special Report on Emission Scenarios
SRTM: Shuttle Radar Topography Mission
SUFI: Sequential Uncertainty Fitting
SWAT: Soil and Water Assessment Tool
SWAT-CUP: SWAT Calibration and Uncertainty Programs
SWHP: Surface Water Hydrology Project
UIB: Upper Indus Basin
UKMO-HadGEM: United Kingdom Meteorological Office, Hadley Centre of Global Environmental Model
UN: United Nations
USA: United States of America
USD: United States Dollar
USGS: United States Geological Survey
WAPDA: Water and Power Development Authority
WMO: World Meteorological Organization

References

1. IPCC. The scientific basis. Cambridge, united kingdom and new york, ny. USA: Cam bridge University Press: 2001.
2. Prasanna, V. Regional climate change scenarios over south asia in the cmip5 coupled climate model simulations. *Meteorol Atmos Phys* **2015**, *127*, 561-578.
3. Zabaleta, A.; Meaurio, M.; Ruiz, E.; Antiguedad, I. Simulation climate change impact on runoff and sediment yield in a small watershed in the basque country, northern spain. *J Environ Qual* **2014**, *43*, 235-245.
4. Velasco, P.P.; Bauwens, W. Climate change analysis of lake victoria outflows (africa) using soil and water assessment tool (swat) and general circulation models (gcms). *Asia Life Sci* **2013**, *22*, 659-675.
5. Aronica, G.T.; Bonaccorso, B. Climate change effects on hydropower potential in the alcantara river basin in sicily (italy). *Earth Interact* **2013**, *17*.

6. Plangoen, P.; Babel, M.S.; Clemente, R.S.; Shrestha, S.; Tripathi, N.K. Simulating the impact of future land use and climate change on soil erosion and deposition in the mae nam nan sub-catchment, thailand. *Sustainability-Basel* **2013**, *5*, 3244-3274.
7. Hormann, G.; Koplin, N.; Cai, Q.; Fohrer, N. Using a simple model as a tool to parameterise the swat model of the xiangxi river in china. *Quatern Int* **2009**, *208*, 116-120.
8. Wang, B.; Lee, J.Y.; Xiang, B.Q. Asian summer monsoon rainfall predictability: A predictable mode analysis. *Clim Dynam* **2015**, *44*, 61-74.
9. Nicholls, R.J.; Marinova, N.; Lowe, J.A.; Brown, S.; Vellinga, P.; De Gusmao, D.; Hinkel, J.; Tol, R.S.J. Sea-level rise and its possible impacts given a 'beyond 4 degrees c world' in the twenty-first century. *Philos T R Soc A* **2011**, *369*, 161-181.
10. Dessai, S.; Hulme, M.; Lempert, R.; Pielke Jr, R. Climate prediction: A limit to adaptation. *Adapting to climate change: thresholds, values, governance* **2009**, 64-78.
11. Mulligan, M. Climate change and food-water supply from africa's drylands: Local impacts and teleconnections through global commodity flows. *Int J Water Resour D* **2015**, *31*, 450-460.
12. Wanders, N.; Van Lanen, H.A.J. Future discharge drought across climate regions around the world modelled with a synthetic hydrological modelling approach forced by three general circulation models. *Nat Hazard Earth Sys* **2015**, *15*, 487-504.
13. Babel, M.S.; Bhusal, S.P.; Wahid, S.M.; Agarwal, A. Climate change and water resources in the bagmati river basin, nepal. *Theor Appl Climatol* **2014**, *115*, 639-654.
14. Park, J.Y.; Park, M.J.; Ahn, S.R.; Park, G.A.; Yi, J.E.; Kim, G.S.; Srinivasan, R.; Kim, S.J. Assessment of future climate change impacts on water quantity and quality for a mountainous dam watershed using swat. *T Asabe* **2011**, *54*, 1725-1737.
15. Booij, M.J.; Tollenaar, D.; van Beek, E.; Kwadijk, J.C.J. Simulating impacts of climate change on river discharges in the nile basin. *Phys Chem Earth* **2011**, *36*, 696-709.
16. Mahmood, R.; Jia, S.F.; Babel, M.S. Potential impacts of climate change on water resources in the kunhar river basin, pakistan. *Water-Sui* **2016**, *8*.
17. Mahmood, R.; Babel, M.S. Evaluation of sdsm developed by annual and monthly sub-models for downscaling temperature and precipitation in the jhelum basin, pakistan and india. *Theor Appl Climatol* **2013**, *113*, 27-44.
18. Archer, D.R.; Fowler, H.J. Using meteorological data to forecast seasonal runoff on the river jhelum, pakistan. *J Hydrol* **2008**, *361*, 10-23.
19. Fowler, H.J.; Archer, D.R. Conflicting signals of climatic change in the upper indus basin. *J Climate* **2006**, *19*, 4276-4293.
20. Pervez, M.S.; Henebry, G.M. Projections of the ganges-brahmaputra precipitation downscaled from gcm predictors. *J Hydrol* **2014**, *517*, 120-134.
21. Reggiani, P.; Rientjes, T.H.M. A reflection on the long-term water balance of the upper indus basin. *Hydrol Res* **2015**, *46*, 446-462.
22. Sharma, V.; Mishra, V.D.; Joshi, P.K. Implications of climate change on streamflow of a snow-fed river system of the northwest himalaya. *J Mt Sci-Engl* **2013**, *10*, 574-587.
23. Höök, M.; Sivertsson, A.; Aleklett, K. Validity of the fossil fuel production outlooks in the ipcc emission scenarios. *Natural Resources Research* **2010**, *19*, 63-81.
24. Hawkins, E.; Sutton, R. The potential to narrow uncertainty in regional climate predictions. *B Am Meteorol Soc* **2009**, *90*, 1095-1107.

25. Räisänen, J.; Palmer, T. A probability and decision-model analysis of a multimodel ensemble of climate change simulations. *J Climate* **2001**, *14*, 3212-3226.
26. Majone, B.; Villa, F.; Deidda, R.; Bellin, A. Impact of climate change and water use policies on hydropower potential in the south-eastern alpine region. *Sci Total Environ* **2016**, *543*, 965-980.
27. Akhtar, M.; Ahmad, N.; Booij, M.J. The impact of climate change on the water resources of hindukush-karakorum-himalaya region under different glacier coverage scenarios. *J Hydrol* **2008**, *355*, 148-163.
28. Arnell, N.W. Effects of ipccsres emissions scenarios on river runoff: A global perspective. *Hydrol Earth Syst Sc* **2003**, *7*, 619-641.
29. FAO. Digital soil map of the world and derived soil properties (version 3.5). **1995**.
30. Ahmad, S.; Mohammad, A.; Khan, S.T. Water tresources of pakistan. **1993**.
31. Dams, W.C.o. *Dams and development: A new framework for decision-making: The report of the world commission on dams*. Earthscan: 2000.
32. Dile, Y.T.; Srinivasan, R. Evaluation of cfsr climate data for hydrologic prediction in data-scarce watersheds: An application in the blue nile river basin. *J Am Water Resour As* **2014**, *50*, 1226-1241.
33. Fuka, D.R.; Walter, M.T.; MacAlister, C.; Degaetano, A.T.; Steenhuis, T.S.; Easton, Z.M. Using the climate forecast system reanalysis as weather input data for watershed models. *Hydrol Process* **2014**, *28*, 5613-5623.
34. Su, B.D.; Zeng, X.F.; Zhai, J.Q.; Wang, Y.J.; Li, X.C. Projected precipitation and streamflow under sres and rcp emission scenarios in the songhuajiang river basin, china. *Quatern Int* **2015**, *380*, 95-105.
35. San Jose, R.; Perez, J.L.; Gonzalez, R.M.; Pecci, J.; Garzon, A.; Palacios, M. Impacts of the 4.5 and 8.5 rcp global climate scenarios on urban meteorology and air quality: Application to madrid, antwerp, milan, helsinki and london. *J Comput Appl Math* **2016**, *293*, 192-207.
36. Hu, Y.R.; Maskey, S.; Uhlenbrook, S. Downscaling daily precipitation over the yellow river source region in china: A comparison of three statistical downscaling methods. *Theor Appl Climatol* **2013**, *112*, 447-460.
37. Fang, G.H.; Yang, J.; Chen, Y.N.; Zammit, C. Comparing bias correction methods in downscaling meteorological variables for a hydrologic impact study in an arid area in china. *Hydrol Earth Syst Sc* **2015**, *19*, 2547-2559.
38. Ouyang, F.; Zhu, Y.H.; Fu, G.B.; Lu, H.S.; Zhang, A.J.; Yu, Z.B.; Chen, X. Impacts of climate change under cmip5 rcp scenarios on streamflow in the huangnizhuang catchment. *Stoch Env Res Risk A* **2015**, *29*, 1781-1795.
39. Ma, C.K.; Sun, L.; Liu, S.Y.; Shao, M.A.; Luo, Y. Impact of climate change on the streamflow in the glacierized chu river basin, central asia. *J Arid Land* **2015**, *7*, 501-513.
40. Bannwarth, M.A.; Hugenschmidt, C.; Sangchan, W.; Lamers, M.; Ingwersen, J.; Ziegler, A.D.; Streck, T. Simulation of stream flow components in a mountainous catchment in northern thailand with swat, using the anselm calibration approach. *Hydrol Process* **2015**, *29*, 1340-1352.
41. Memarian, H.; Balasundram, S.K.; Abbaspour, K.C.; Talib, J.B.; Sung, C.T.B.; Sood, A.M. Swat-based hydrological modelling of tropical land-use scenarios. *Hydrolog Sci J* **2014**, *59*, 1808-1829.
42. Saha, P.P.; Zeleke, K.; Hafeez, M. Streamflow modeling in a fluctuant climate using swat: Yass river catchment in south eastern australia. *Environ Earth Sci* **2014**, *71*, 5241-5254.
43. Chiang, L.C.; Yuan, Y.P.; Mehaffey, M.; Jackson, M.; Chaubey, I. Assessing swat's performance in the kaskaskia river watershed as influenced by the number of calibration stations used. *Hydrol Process* **2014**, *28*, 676-687.

44. Arnold, J.G.; Srinivasan, R.; Muttiah, R.S.; Williams, J.R. Large area hydrologic modeling and assessment part i: Model development1. Wiley Online Library: 1998.
45. Haguma, D.; Leconte, R.; Cote, P.; Krau, S.; Brissette, F. Optimal hydropower generation under climate change conditions for a northern water resources system. *Water Resour Manag* **2014**, *28*, 4631-4644.
46. Park, J.Y.; Kim, S.J. Potential impacts of climate change on the reliability of water and hydropower supply from a multipurpose dam in south korea. *J Am Water Resour As* **2014**, *50*, 1273-1288.
47. Rahman, K.; Maringanti, C.; Beniston, M.; Widmer, F.; Abbaspour, K.; Lehmann, A. Streamflow modeling in a highly managed mountainous glacier watershed using swat: The upper rhone river watershed case in switzerland. *Water Resour Manag* **2013**, *27*, 323-339.
48. Ahmad, Z.; Hafeez, M.; Ahmad, I. Hydrology of mountainous areas in the upper indus basin, northern pakistan with the perspective of climate change. *Environ Monit Assess* **2012**, *184*, 5255-5274.
49. Butts, M.B.; Payne, J.T.; Kristensen, M.; Madsen, H. An evaluation of the impact of model structure on hydrological modelling uncertainty for streamflow simulation. *J Hydrol* **2004**, *298*, 242-266.
50. Srinivasan, R.; Zhang, X.; Arnold, J. Swat ungauged: Hydrological budget and crop yield predictions in the upper mississippi river basin. *T Asabe* **2010**, *53*, 1533-1546.
51. Teshager, A.D.; Gassman, P.W.; Secchi, S.; Schoof, J.T.; Misgna, G. Modeling agricultural watersheds with the soil and water assessment tool (swat): Calibration and validation with a novel procedure for spatially explicit hrus. *Environ Manage* **2016**, *57*, 894-911.
52. Singh, D.; Gupta, R.D.; Jain, S.K. Assessment of impact of climate change on water resources in a hilly river basin. *Arab J Geosci* **2015**, *8*, 10625-10646.
53. Ligaray, M.; Kim, H.; Sthiannopkao, S.; Lee, S.; Cho, K.H.; Kim, J.H. Assessment on hydrologic response by climate change in the chao phraya river basin, thailand. *Water-Sui* **2015**, *7*, 6892-6909.
54. Deb, D.; Butcher, J.; Srinivasan, R. Projected hydrologic changes under mid-21st century climatic conditions in a sub-arctic watershed. *Water Resour Manag* **2015**, *29*, 1467-1487.
55. Neitsch, S.; Arnold, J.; Kiniry, J.e.a.; Srinivasan, R.; Williams, J. Soil and water assessment tool user's manual version 2000. *GSWRL report* **2002**, *202*.
56. Smith, J.B.; Schneider, S.H.; Oppenheimer, M.; Yohe, G.W.; Hare, W.; Mastrandrea, M.D.; Patwardhan, A.; Burton, I.; Corfee-Morlot, J.; Magadza, C.H. Assessing dangerous climate change through an update of the intergovernmental panel on climate change (ipcc)"reasons for concern". *Proceedings of the National Academy of Sciences* **2009**, *106*, 4133-4137.
57. Hashmi, H.N.; Siddiqui, Q.T.M.; Ghumman, A.R.; Kamal, M.A.; Mughal, H. A critical analysis of 2010 floods in pakistan. *Afr J Agr Res* **2012**, *7*, 1054-1067.
58. Ziegler, A.D.; Lim, H.; Tantasarin, C.; Jachowski, N.R.; Wasson, R. Floods, false hope, and the future. *Hydrol Process* **2012**, *26*, 1748-1750.